Magma degassing during subglacial eruptions and its use to reconstruct palaeo-ice thicknesses

Hugh Tuffen*

Jacqueline Owen [j.owen2@lancaster.ac.uk]

Joanna S. Denton [jo.denton@lancaster.ac.uk],

Lancaster Environment Centre, Lancaster University, LA1 4YQ, UK

*Corresponding author. Email h.tuffen@lancaster.ac.uk

Phone +44 [0]1524 594713

Fax +44 [0]1524 593975

Abstract

The degassing of magmatic volatiles during eruptions beneath ice sheets and glaciers, as recorded by the dissolved volatile content quenched in volcanic rocks, could provide powerful new constraints on former ice thicknesses in volcanic areas. As volcanic rocks are readily dateable using radiometric methods, subglacial volcanoes may therefore provide crucial information on the timing of palaeo-environmental fluctuations in the Quaternary. Volatile degassing is also likely to control the mechanisms of subglacial eruptions and their associated hazards.

In this paper we lay out a number of criteria that must be satisfied for degassing to potentially record palaeo-ice thicknesses, using a variety of new datasets and calculations to highlight existing problems with the technique. These include uncertainties about volatile solubilities, non-equilibrium degassing, sample heterogeneity, hydration, post-quenching movement and whether subglacial pressures deviated significantly from glaciostatic. We propose new strategies for improvement of the technique and discuss how magmatic volatiles may control the style of subglacial eruptions.

Keywords

Subglacial eruptions; glaciovolcanism, ice sheet; palaeoenvironments, magma, degassing, Iceland, British Columbia, hyaloclastite, pillow lava, tuya, tindar

1. Introduction

Volcanoes that have interacted with ice provide a valuable palaeo-environmental record, as the nature of deposits formed (e.g. subglacial-subaerial transitions) may be used to reconstruct approximate ice thicknesses (e.g. Smellie, 2000; Smellie, 2008; Smellie et al., 2008). Indeed, as volcanic rocks are readily datable through radioactive decay series they may provide a unique opportunity to track the history of how ice sheets have fluctuated during past global climate change (Smellie et al., 2008).

However, many subglacially erupted formations do not provide any clear evidence for approximate ice surface elevations – especially those that erupted entirely beneath the ice (e.g. Skilling, 1994; Tuffen et al., 2001; Dixon et al., 2002; Schopka et al., 2006; McGarvie et al., 2007; Edwards et al., 2009). In these cases the pressure-dependent solubility of magmatic volatiles may potentially be used to estimate palaeo-pressures at the eruption site, which may provide information on both palaeo-ice thicknesses and the local subglacial hydrology.

The degassing of magmatic volatiles during subglacial eruptions (principally H_2O, CO_2, S, F and Cl) may strongly influence eruptive mechanisms and associated hazards, as is the case with subaerial eruptions (Sparks, 2003; Edmonds, 2008). Additionally, volatile degassing controls the emission of climate-affecting gases such as CO_2 and SO_2 into the oceans and atmosphere (Gíslason et al., 2002; Edmonds, 2008). As melting of ice sheets may promote subglacial volcanic activity (Maclennan et al., 2002; Pagli and Sigmundsson, 2008) there is therefore scope for feedback between climate change and patterns of subglacial volcanism (Huybers and Langmuir, 2009).

In this paper we present a critical overview of the use of volatile contents in subglacially erupted glasses to reconstruct palaeo-ice thicknesses. New data is

provided that highlights the strong heterogeneities in volatile contents within samples that may seriously hamper use of the technique. We then systematically outline the criteria that must be met by samples in order for quenching pressures to be recorded, before discussing the interpretation of quenching pressures and their relationship to palaeo-ice thicknesses. Finally, the potential effect of volatiles on the mechanisms of eruptions is described, along with key topics for future research.

1.1. Previous studies of degassing: subglacial basaltic eruptions

To date studies of volatile degassing at subglacial volcanoes have concentrated on Icelandic and British Columbian examples (Table 1). Studies involved measurement of the dissolved volatile contents in glassy samples collected from different elevations at subglacially erupted tuyas (that pierced the ice surface and became subaerial) and tindar ridges (that remained entirely subglacial). A schematic diagram of magma degassing and vesiculation during eruptions is given in Fig. 1; see Smellie (2000) for detailed definitions of eruption types.

In the first study to use magmatic volatile contents as a method to estimate the palaeo-ice thickness, Dixon et al. (2002) looked at degassing at Tanzilla Mountain, British Columbia – an entirely englacial volcanic edifice composed of alkali basalt overlying a base of tholeiitic pillow lavas. H_2O, S and Cl data showed that although the tholeiitic base had not significantly degassed the overlying alkali basalt had done so. Pressure-solubility relations for basaltic magma (Dixon and Stolper, 1995) were to estimate the confining pressure consistent with the measured H_2O concentrations; this led to the estimate that 400-900 m of ice lay over the vent during the eruption. This range of figures was roughly consistent with independent estimates of the ice sheet thickness.

Schopka et al. (2006) measured the water contents of samples from the base to the summit of Helgafell, a small-volume, 330 m-high Pleistocene basaltic tindar ridge in western Iceland. Surprisingly, no systematic relationship between water content and elevation was found and the low water contents (0.26-0.37 wt %) were consistent with lower quenching pressures than expected (equivalent to only 90-180 m of ice). The authors speculated that meltwater drainage may lead to confining pressures considerably less than glaciostatic, so that the magma did not feel the full weight of the overlying ice when it quenched at the vent.

Hoskuldsson et al. (2006) found high water contents (0.85-1.04 wt %) in Pleistocene pillow lavas at Kverkfjoll, Iceland, which were consistent with eruption between 1240 and 1880 m of ice. As Kverkfjoll is located in the centre of Iceland where the ice thickness may have reached 2 km during glacial periods this range of values is realistic. Hoskuldsson et al. also used the vesiculation of some pillow lavas to argue that a sudden decrease in subglacial pressure occurred, due to the release of subglacial meltwater in a jökulhlaup flood.

Edwards et al. (2009) found high magmatic water contents in basaltic pillow lavas at Mt Edziza, British Columbia that make up an englacially erupted ridge. They found significant variations in volatile content with elevation, but there was no simple trend, and so suggested that the level of an ice-confined lake may have fluctuated during the eruption.

1.2. Previous studies of degassing: subglacial intermediate and silicic eruptions

Studies to date of degassing during subglacial silicic eruptions have been restricted to Icelandic examples. McGarvie et al. (2007) measured water contents in rhyolitic lavas at Prestahnúkur, a 600 m-high subglacially erupted edifice dominated by lava flows.

Low water contents (0.10-0.14 wt %) were attributed to low-pressure degassing at the vent followed by substantial downslope flow. Tuffen et al. (2008) found elevated water contents (0.50-0.52 wt %) in glass from Dalakvísl, Torfajökull consistent with partial degassing during an explosive eruption within an subglacial cavity.

In the only study of intermediate magma to date Stevenson et al. (2009) found high water contents (0.67-1.32 wt %) in andesitic and dacitic glasses from Kerlingafjöll central volcano. As the highest water content measured required unrealistically thick ice (>3 km), it was attributed to loading by thick ice and pyroclastic deposits. Tuffen and Castro (2009) traced degassing from the feeder dyke to subaerial rhyolitic lavas erupted through thin ice/firn at Hrafntinnuhryggur, Krafla. They found that subaerial lavas were degassed but with substantial small-scale heterogeneity (0.11-0.20 wt % H_2O) and the inferred quenching pressure from water contents in the feeder dyke was too high to be explained by loading by ice/firn alone.

Denton et al. (2009) studied the post-emplacement hydration of rhyolitic lavas and hyaloclastites from Torfajökull and Krafla and found that perlitisation and zeolite alteration due to high-temperature interactions with meltwater could increase total volatile contents from ~1 wt % to as much as 9 wt %.

2. The use of volatile degassing to reconstruct quenching pressures: essential criteria

In this section we present a new framework for the use of volatiles to reconstruct quenching pressures during subglacial eruption, and systematically address the key criteria that must be met by samples for the technique to yield robust results.

2.1. Volatile-saturated magma

Magma degasses as it rises from the chamber to the surface if the pressure decrease during its ascent is sufficient to create volatile oversaturation (e.g. Wilson, 1980). This then leads to the exsolution of dissolved volatiles from the melt phase into vapour/fluid within bubbles (e.g. Sparks, 1978), which leads to a decrease in the concentration of volatiles remaining in the melt. In order for the dissolved volatile content remaining in a melt to record the confining pressure it is essential for some degassing to have occurred, so that there has been the chance for volatile diffusion into bubbles to keep track with any decrease in confining pressure. Therefore only volatile-saturated samples that have undergone some degassing should be used to reconstruct quenching pressures. Samples that have not degassed can only indicate minimum quenching pressures.

Indicators that volatile-saturated melt has been erupted come from both textures and geochemistry. The presence of vesicles in glasses (Fig. 2a) is taken to be diagnostic as it indicates that conditions for bubble nucleation and growth were reached (e.g. Schopka et al., 2006). However, vesicles may collapse and thoroughly heal (Westrich and Eichelberger, 1994), so the absence of vesicles does not necessarily indicate the melt was undersaturated. In lavas care must be taken not to confuse vesicles formed through volatile exsolution with cavities generated by late-stage brittle-ductile magma deformation (e.g. Smith et al., 2001). An important complication is that the solubility of different volatile species differs greatly. For example, CO_2 is much less soluble than H_2O in silicate glasses (e.g. Johnson et al. 1994), so initial degassing may result in CO_2 loss into vesicles with little loss in H_2O. This means that vesicular glasses can form without the occurrence of significant H_2O degassing. Geochemical evidence that degassing has occurred comes from comparing

the concentration of volatile species such as H_2O with incompatible elements such as K_2O (e.g. Dixon et al., 2002; Nichols et al., 2002). As the concentration of both species can increase through crystallisation a linear H_2O-K_2O trend is typically found in magma suites (e.g. Nichols et al., 2002). Samples less water-rich than the linear trend are those that have degassed.

Subglacial volcanic successions have typically degassed to some extent, with pillow lavas, hyaloclastites and lava bodies almost invariably containing vesicles, but one exception is reported in the literature: the tholeiitic unit at the base of Mt Tanzilla, British Columbia (Dixon et al., 2002). Nichols et al. (2002) also found that submarine pillow lavas on the Reykjanes Ridge had not degassed, in contrast with subglacial pillow lavas in Iceland.

An interesting implication is that the initial volatile content of the magma may restrict the maximum ice thickness it is possible to reconstruct from degassing. This restriction is most likely to apply to basaltic magmas, which typically have lower initial volatile contents than rhyolitic magmas (Johnson et al., 1994). Degassing of water from mid-ocean-ridge basalts only occurs beneath at most a few hundred metres of water (Moore, 1970), whereas explosive pumice-producing eruptions of rhyolitic magma driven by water exsolution from melt may occur beneath water 1-2 km deep (e.g. Wright et al., 2003). Volatile-rich rhyolitic eruptions can therefore be expected to provide a better record of palaeo-ice thicknesses than basalts when ice exceeds several hundred metres in thickness, although the volatile content of both rhyolites and basalts depends strongly on the tectonic setting (Johnson et al., 1994).

The initial volatile content of magma recorded in primary melt inclusions should ideally be determined as this provides a complete picture of degassing from the

chamber to the surface. Surprisingly, to date no published study of magma degassing in subglacial eruptions has included melt inclusion data.

2.2. Equilibrium degassing

It is only possible to infer quenching pressures from the dissolved volatile contents in volcanic glasses if equilibrium degassing has occurred. The pressure-solubility experiments that underpin our understanding of how rising magma degasses are based on equilibrium exchange between the volatiles dissolved in the melt and present as vapour or fluids in bubbles. Although it was long assumed that volatile degassing during magma ascent was always in equilibrium with the confining pressure (e.g. Wilson, 1980), most recent models have shown that non-equilibrium degassing may be important (e.g. Proussevitch and Sahagian, 1996). Non-equilibrium degassing is also apparent in MORB glasses, which tend to be supersaturated, indicating that the kinetics of bubble nucleation and growth, driven by exsolution of CO_2, are too slow to maintain melt-vapour equilibrium during magma ascent (Fine and Stolper, 1986; Stolper and Holloway, 1988; Dixon et al., 1988; 1995). Supersaturation is rarely observed in basalts with greater than 0.4 wt% H_2O, however, as higher water concentrations promote faster diffusion rates allowing bubble growth to keep pace with magma ascent (Simons et al., 2002).

Non-equilibrium degassing occurs when the exsolution of volatiles into growing bubbles is held back by sluggish bubble nucleation, viscous resistance to decompressive bubble growth or slow volatile diffusion into bubbles. The consequent delay in adjusting the amount of dissolved volatiles in the melt to a change in confining pressure can lead to an oversaturation of volatiles in the melt. Using models of coupled diffusive-decompressive bubble growth in magmas, Proussevitch and

Sahagian (1996) have found that there is a threshold magma ascent rate above which equilibrium degassing is unlikely to occur. This value is much lower for rhyolitic magmas (~1 m s^{-1}) than basaltic magmas (>100 m s^{-1}) as bubble growth and volatile diffusion are more strongly retarded by the higher viscosity of rhyolitic melt.

In order to know whether subglacially erupted glasses underwent equilibrium degassing it is therefore necessary to estimate the magma ascent rate. For basaltic magma it is thought that only the most violent phreatomagmatic eruptions involve sufficiently fast ascent rates (in excess of 100 m s^{-1}) to lead to non-equilibrium degassing (Mastin et al., 2004). Therefore one can be confident that almost all subglacial basaltic glasses (the margins of pillows, lavas, dykes, intrusions and quench hyaloclastites) will have undergone equilibrium degassing. The only possible exception is hyalotuffs formed during exceptionally violent magma-water interactions.

Rhyolitic magma, in contrast, will tend to undergo non-equilibrium degassing unless magma ascent rates are less than 1 m s^{-1}. Plinian explosive eruptions are likely to involve far higher magma ascent rates (Wilson, 1980), whereas new petrological data shows that subplinian and effusive eruptions may involve far lower average ascent rates of <0.02 m s^{-1} (Castro and Gardner, 2008). It must be noted, however, that these are average ascent rates over a ~4 km long conduit and final ascent rates prior to fragmentation and quenching in the upper ~500 m of the conduit will be significantly higher than this average value. Therefore any explosively erupted rhyolitic deposit should be treated with caution, unless there is good evidence that the deposit may have cooled sufficiently slowly for re-equilibration to occur, e.g. the development of substantial rheomorphic welding within pyroclastic deposits (Tuffen et al., 2008).

The ascent rate of rhyolitic magma rising in a dyke (Fig. 2b) can be approximated from the following expression for buoyant magma rise through the Icelandic crust, adapted from equation 7 of Hoskuldsson and Sparks (1997):

$$v = \frac{(\rho_c - \rho_m) g h^2}{3\mu}$$

where v is the magma rise velocity in m s^{-1}, ρ_c is mean crustal density over the dyke length (2700 kg m^{-3}), ρ_m is magma density (2300 kg m^{-3}), g is the acceleration due to gravity (9.81 m s^{-2}), h is the dyke half-width in m and μ is the magma shear viscosity in Pa s.

Reasonable values of h and μ for Icelandic eruptions are 2-10 m and 10^6-10^7 Pa s respectively, providing a range of ascent rates of 0.001–0.27 m s^{-1}, which falls well within the range for equilibrium degassing and independent estimates of ascent rates from decompression experiments (Castro and Gardner, 2008). Therefore one can be confident that products of effusive subglacial rhyolite eruptions, such as lava lobes, lava flows, quench hyaloclastites and feeder dykes, have undergone equilibrium degassing.

2.3. Lack of post-quenching movement

If a sample has degassed or quenched at one elevation but then subsequently moved to another elevation it may provide misleading information about the thickness of overlying ice. For example, a lava flow may degas to atmospheric pressure if an eruption has melted through the ice surface, but then flow a considerable distance down the volcano flanks beneath a substantial thickness of ice (Fig. 3a; McGarvie et

al., 2007). Such lava may be degassed to near atmospheric pressure but found near the base of a subglacial edifice erupted beneath thick ice. The greater the distance a lava can flow subaerially the closer it can come to being fully degassed to atmospheric pressure (Moore et al., 1995). Therefore when selecting a lava body to sample one must assess from field relationships whether it may have flowed a significant distance downslope from the vent (Fig. 3b).

There may also be considerable vertical movement of individual clasts in any hydroclastic rocks formed during explosive magma-water interaction or deposited within a meltwater lake, as well as uncertainty about quenching depths. Quenching during phreatomagmatic activity may occur at a depth of tens to hundreds of metres in the conduit if external water is able to interact with magma at that depth (Mastin et al., 2004). Therefore clasts within hyalotuffs formed during explosive magma-water interaction may not quench at the base of the ice but some depth beneath it, and the quenching pressures recorded by volatile degassing may not indicate the hydrostatic pressure. Even if magma-water interaction only commenced once rising magma encountered a body of meltwater at the base of the ice there could still be considerable uncertainty about where quenching occurred if the meltwater depth were significant (Fig. 3c). This is because individual clasts may quench during their trajectory within the body of meltwater (Guðmundsson, 2003), which may be many tens of metres, during which the confining pressure will change.

Post-quenching movement of clastic material (Fig. 3c) is almost inevitable during deposition and will be most important when deposition occurs through a deep column of meltwater. Even in near-vent concentrated mass flow deposits where individual clasts do not enter a body of meltwater mass movement of material may involve significant changes in elevation. Post-depositional movement may also occur,

for example due to edifice instability triggered by meltback of supporting ice walls, with downslope slumping of poorly or well-consolidated hyaloclastites (Skilling, 1994; Tuffen et al., 2001). The only clastic material likely to have quenched in-situ is breccias formed by at the margins of lava bodies, including peperites (e.g. Tuffen et al., 2001; Smellie, 2008).

2.4. Homogeneous samples

An important question is therefore whether the volatile content of the volume analysed is representative of the degassing behaviour of the whole sample or whether it is influenced by small-scale processes that create inhomogeneous volatile contents. Recent microanalytical studies have revealed the extent to which water and other volatile species may be spatially heterogeneous in vesicle- and crystal-bearing glasses (Castro et al., 2005; Castro et al., 2008). The heterogeneity may be due to frozen-in diffusion gradients around bubbles and crystals or within welded breccias (Rust and Cashman, 2007).

For example, late-stage spherulite crystallisation in obsidian erupted through thin ice at Hrafntinnuhryggur, Krafla, Iceland has caused localised volatile enrichment in the residual melt (Castro et al., 2008). Glass water contents increase from "background" values of 0.10-0.14 wt % far from spherulites to ~0.20 wt % at the edge of spherulites. As spherulite crystallisation is a late-stage disequilibrium process that can locally increase melt volatile contents it is obvious that the "background" water concentrations are those that should be used to estimate the quenching pressure. However in highly vesicular samples there may be no homogenous "background" volatile concentration as diffusion gradients from neighbouring bubbles overlap (Tuffen, unpublished data 2009). In this case it is far from obvious which volatile

concentration should be taken as representative of the sample and bulk extraction techniques, which provide an average volatile concentration for milligrams to grams of sample may be preferable, although results may be strongly affected by hydration (see following section).

Therefore the most robust results will come from studies where multiple analyses have been first carried out to determine the degree of small-scale volatile heterogeneity in samples. It is only then that there is the potential for measured volatile contents to reliably indicate quenching pressures.

In sections 3.3 and 3.4 we present data highlighting the strong heterogeneity in magmatic volatiles that may occur in subglacially erupted glasses.

2.5. Lack of post-quenching hydration

Subglacial eruptions typically involve extensive interactions with meltwater both during and after activity (e.g. Guðmundsson et al., 2004; Jarosch et al., 2008). Post-eruptive hydration of clastic subglacial deposits by meltwater is therefore commonplace and basaltic hyaloclastites are almost always palagonitised, which involves hydration by meteoric water (Jakobsson, 1978). Similarly rhyolitic fragmental deposits are likely to be hydrated and perlitised (Denton et al., 2009). As water is the volatile species most commonly used to reconstruct quenching pressures care must be taken to avoid hydrated samples.

There are five methods that can be used to identify hydrated samples. (1) The isotopic composition of water can be measured by coupling a bulk extraction technique to high-resolution mass spectrometry (DeGroat Nelson et al., 2001). This can distinguish between magmatic and meteoric volatile signatures, but the technique

is yet to be applied to any subglacially erupted deposit. It is the most reliable technique.

(2) A microanalytical technique such as ion or electron microprobe or infra-red microspectroscopy may be used to map the spatial distribution of volatile contents in a sample and thus identify parts of a sample that have not been hydrated. (3) The speciation of water can be determined using infrared spectroscopy. Hydrated water tends to remain as molecular H_2O whilst magmatic water, when present in small concentrations (<1 wt %) is dominated by hydroxyl and silanol groups (Ihinger et al., 1994; Zhang, 1999). This technique is not infallible as the speciation of magmatic water is concentration- and cooling-rate dependent, but it can act as a useful guide. (4) Hydrated samples tend to dehydrate at lower temperatures than non-hydrated samples during bulk extraction techniques such as thermogravimetric analysis (Denton et al., 2009; Stevenson et al., 2009). Figure 4 shows the temperature of most rapid water loss during heating of subglacially erupted rhyolite glasses to 1250 °C in a thermogravimetric analyser (Denton et al., 2009). There is a strong inverse relationship between the total volatile content, which is an approximate index of hydration, and the temperature of fastest degassing. This relationship indicates that hydrated water is more weakly bound to the silicate framework than magmatic water and can be used to identify hydrated samples. (5) Hydration of glasses may create distinctive textures such as perlitic fracturing in rhyolites (Denton et al., 2009) or distinctive colouration (palagonitised basaltic glass is paler than fresh non-hydrated glass). Although this criterion is the most readily applied and can be used in the field it is not infallible as incipient hydration may not produce any obvious textures (Denton et al., in preparation). It is therefore recommended that method (5) is used in

addition to other quantitative methods. The extent to which the concentration of other volatile species can be affected by hydration and alteration is not currently known.

New data indicating heterogeneous hydration of subglacially erupted rhyolitic glasses on two different spatial scales is presented in the following section.

3. Case studies of volatiles in subglacially erupted rhyolitic glasses from Torfajokull, Iceland

We present data on the extent of volatile heterogeneity over different spatial scales in rhyolitic glasses from Torfajokull, Iceland. The heterogeneity may be due either to variability in magmatic volatile contents or variable degrees of hydration by meltwater and has profound implications for which samples are suitable for reconstructing palaeo-ice thicknesses and for how volatile concentrations are interpreted.

3.1. Hydration – outcrop scale

Rhyolitic lava lobes surrounded by quench hyaloclastite breccia were generated during an effusive subglacial eruption at Bláhnúkur, Torfajokull, Iceland (Tuffen et al., 2001; 2002a). Lobes are characterised by gradational contacts with the hyaloclastite breccia, indicative of quench fragmentation during high-temperature lava-meltwater interaction. The perlitic textures found in hyaloclastite and the lava lobe margins indicate that hydration occurred during these interactions (Denton et al., 2009). To examine the extent of hydration of glass by meltwater samples were collected from lava lobe B120 at 63°58'50.0" N, 19°03'15.1" W at 780 m elevation on the eastern flank of Bláhnúkur. Samples were taken from transect between the non-perlitised lava interior and the perlitised, quench-fractured margin (Fig. 5).

The total volatile content of bulk samples was determined using a TA Instruments SDT Q600 simultaneous differential scanning calorimetry – thermal gravimetric analyser (DSC-TGA) instrument coupled to an HPR-20 QIC Gas Analysis System at Lancaster University. The furnace was purged by oxygen-free N_2 during measurements. Samples were crushed and sieved, the 125-500 μm size fraction was washed with acetone and then oven-dried at 110 ºC for ~1 hour prior to analysis, following the method of Newman et al. (1986). Approximately 30 mg of sample was then heated in platinum cups at 5 ºC min^{-1} from ambient temperatures to 1250 ºC, which was sufficient to thoroughly degas all volatile species. Mass spectrometer counts did not give quantitative concentrations of the different volatile species detected (H_2O, CO_2, F, Cl, SO_2) but demonstrated that water was by far the most abundant volatile species (Denton et al., 2009). At least one duplicate of each sample was measured and average results presented.

Total volatile content data is provided in Fig. 5 and Table 2. Over a distance of 33 cm the total volatile contents, which are dominated by water, increase strongly from 1.06 to 1.96 wt %. This indicates progressive hydration from the near-pristine glass of the lava lobe interior to the surrounding, strongly-perlitised hyaloclastite, consistent with the invasion of meltwater into crack networks in the cooling lava. In order to reconstruct quenching pressures from magmatic water contents it is therefore essential to sample the freshest, least hydrated glass possible from such an outcrop. As textures formed by incipient hydration and perlite formation may be difficult to identify (Denton et al. in preparation), it is therefore advisable to collect and analyse multiple samples from each locality.

3.2. Hydration – sample scale

Hydration may also create considerable variations in volatile content within individual samples, over a scale of hundreds of microns to millimetres. We have measured spatial variations in water content within a sample of perlitised rhyolitic lava from Bláhnúkur. The sample was collected from the margin of an intrusive lava body within perlitised hyaloclastite at 775 m elevation (63°58' 44.6" N, 19°03'42.5" W), on Bláhnúkur's western flank. Water contents were measured using the Thermo Nicolet Fourier transform infrared spectrometer (FTIR) at The Open University, UK. A liquid N_2-cooled MCT-A detector and KBr beamsplitter was used, with a spot size of 45 x 45 μm. The sample chamber was purged with dried air and 256 scans were taken between 5000 and 1000 cm^{-1}. Samples were mounted to glass slides using Crystalbond® resin and hand polished on both sides. Their thicknesses (~100-200 μm) were measured using a Mitutoyo digital displacement gauge, with an error of ± 5 μm. The intensities of the -OH_T and -OH absorption peaks at 3550 cm^{-1} and 4530 cm^{-1} were used to calculate water contents using the Beer-Lambert law, a linear baseline correction and absorption coefficients given by Ihinger et al. (1994). No CO_2 peak was detectable. The water concentration was measured over a transect between the centre and margin of a perlitic bead ~500 μm in diameter.

Measured water contents are shown in Fig. 6, indicating strong gradients in water content on a 10-100 micron scale. These indicate variable degrees of hydration associated with different distances from the bead margin, consistent with the idea that water ingress occurs along the fractures bounding beads (Denton et al., 2009). The bead centre is not significantly hydrated, meaning that the magmatic volatile content can here be measured. If a micro-analytical technique is being used to measure volatile contents and there is any evidence that hydration may have occurred (such as

433 the presence of cracks), it is advisable to collect multiple measurements from different
434 positions in the sample to determine the spatial distribution of hydration.
435
436 **3.3. Small-scale heterogeneity in magmatic volatiles: H_2O in rhyolitic glass**
437 Small-scale heterogeneities in magmatic concentrations have recently been discovered
438 in subaerially erupted rhyolitic glasses and melt inclusions, associated with vesicle
439 growth and leakage of inclusions (Castro et al., 2005; Humphreys et al., 2008).
440 Similar heterogeneities have also been identified in subglacially erupted obsidian
441 from Hrafntinnuhryggur, Krafla, Iceland (Castro et al., 2008), which were attributed
442 to late-stage spherulite crystallisation.
443 Subglacially erupted rhyolite glasses are commonly texturally heterogeneous,
444 with the development of flow banding and welded breccia textures (Tuffen et al.,
445 2003). To ascertain whether this can create heterogeneous volatile concentrations the
446 water content within a sample of welded obsidian breccia was mapped. The sample
447 was collected from a shallow dissected conduit at SE Rauðfossafjöll rhyolitic tuya,
448 Torfajökull, Iceland (Tuffen et al., 2002b; Tuffen and Dingwell, 2005). Measurements
449 were conducted using a Nicolet Model 800 infra-red spectrometer at the University of
450 Bristol (Tuffen, 2001). Pea-sized samples of obsidian were mounted on a glass slide
451 with dental resin, and double-polished to thicknesses of 100-600 μm. Thicknesses
452 were measured with a Mitutoyo digital micrometer, with an accuracy of 5 μm.
453 Analyses were carried out in a chamber purged with nitrogen, and background counts
454 were made between every 3-4 analyses. A square beam of 50 μm width was used. The
455 height of the absorbance peak at 3550 cm^{-1} (total water, e.g. Zhang, 1999), was used
456 to calculate the water content, using the correlation coefficient of Newman et al.,
457 (1988). Cumulative errors from uncertainties in measurements and the absorption

458 coefficient are about 10%. No CO_2 absorption peaks were seen, indicating that CO_2
459 concentrations were below the detection limits of ~30 ppm.
460 Results (Fig. 7) confirm that strong heterogeneity in water content is present,
461 from 0.12 to 0.27 wt %, due to the juxtaposition of variably degassed fragments of
462 magma during emplacement of the lava. Similar variations have been identified in
463 welded pyroclastic obsidian samples from subaerial eruptions (Rust and Cashman,
464 2007). This poses a difficult question: which of this range of water concentrations is
465 representative of the sample? The heterogeneity is due to variable amounts of
466 degassing, rather than the ingress of external water, but which if any of the volatile
467 contents best represents the pressure of quenching? As shallow brittle-ductile
468 processes such as those generating these textures can involve significant changes in
469 confining pressure and weld together clasts with different degassing histories it is
470 wise to avoid such heterogeneous samples when seeking to reconstruct quenching
471 pressures, and thus palaeo-ice thicknesses.
472 Rhyolitic glasses have a much stronger tendency than basaltic glasses to
473 contain strong spatial heterogeneities in magmatic water contents, due to the more
474 sluggish diffusion of water through the melt (Zhang, 1999). Therefore these problems
475 are less likely to apply to basaltic glasses.
476
477 **3.4. Small-scale heterogeneity in magmatic volatiles: fluorine**
478 To determine whether other volatile species concentrations are also spatially
479 heterogeneous, we have carried out a study of fluorine concentrations in a sample of
480 flow-banded subglacially erupted rhyolitic obsidian from Bláhnúkur. The sample,
481 collected from the non-perlitic interior of lava lobe J2 at 710 m elevation (63°58'
482 58.7" N, 19°03'43.6" W) contains five distinctive colours of flow band (Fig. 8). Major

element and halogen concentrations were determined using a Cameca SX-100 electron microprobe at the University of Cambridge and data are presented in Table 3. The analytical conditions used were optimised to minimise sodium loss, with an accelerating voltage of 15 keV, beam current of 4 nA and spot size of 10 μm.

Figure 8 shows that strong spatial variations in fluorine contents exist, both between and within flow bands. As other species are far less variable (Table 3) this is attributed to heterogeneous degassing rather than mixing of magmas with contrasting compositions. Ductile processes such as the growth and collapse of vesicles can therefore also create considerable spatial variations in magma volatile contents. If fluorine contents were used to estimate quenching pressures each flow band would yield very different results and again there is the difficult question of which one value, if any, can be taken as representative of the sample.

4. Estimation of quenching pressures from volatile concentrations

Once robust volatile concentration data for suitable samples has been gathered this can be used to estimate the pressure at which samples quenched. Although the solubility of all volatile species in magma is pressure-dependent (e.g. Blank and Brooker, 1994; Carroll and Webster, 1994; McMillan, 1994) water is currently the most useful and widely employed as its pressure-dependent solubility is well documented and it degasses over a range of pressures relevant to the load exerted by ice sheets and glaciers. The discussion below will therefore focus on the solubility of water as it is to date the only species used to estimate quenching pressures.

4.1. Solubility-pressure relationships for water

Recent experimental studies have determined the pressure-dependent solubility of water in magma spanning a wide range of magma compositions, temperatures, pressures and water contents (summarised in McMillan, 1994; Zhang, 1999). This allows measured magmatic water contents to be converted to confining pressures if it is assumed that degassing was in equilibrium.

There are many different formulae that can be used to calculate solubility pressures from water contents, which result from numerous studies on different magma compositions (e.g. Dixon and Stolper, 1995; Dixon et al., 1997; Moore et al., 1998; Papale et al., 2006) or have been subsequently derived from them (e.g. Mastin et al., 2004). The formulae used in previous studies of subglacial degassing are indicated in Table 1. Due to its ease of use the most commonly employed is VolatileCalc (Newman and Lowenstern, 2002). This allows any measured water content to be converted to a solubility pressure for either rhyolitic or basaltic magma, once the magma temperature and CO_2 content are specified. As water solubilities are strongly composition-dependent (e.g. solubilities in tholeiitic and alkalic basalts are different) grouping all magmas into rhyolitic or basaltic can introduce considerable error.

For intermediate magmas other models are therefore more appropriate, so in their study of andesite and dacite degassing Stevenson et al. (2009) used the models of Moore et al. (1998) and Papale et al. (2006). Another source of error when using VolatileCalc is that the computational parameters used make solutions only approximate at the low water contents (<1 wt %) typical of subglacial glasses (J. Lowenstern, pers. comm. 2008).

The solubility-pressure curves for water in rhyolitic and basaltic magmas calculated using VolatileCalc is shown in Figure 9. For rhyolitic magmas (Fig. 9a)

there is little difference between the curves for magma at 850 and 950 °C, which spans the common range of eruptive temperatures, meaning that uncertainty about the eruptive temperature does not introduce significant error into the pressure estimates. The equivalent data for basalts (Fig. 9b) similarly shows relative insensitivity to eruption temperatures.

4.2. The CO_2 problem and the halogens

A major source of uncertainty in pressure estimates comes from the influence CO_2 concentrations exert on the saturation value of water (e.g. Liu et al., 2005). The addition of only tiny quantities of CO_2 to a melt (several to tens of ppm) strongly decreases the saturation value of water by reducing the water fugacity in vapour phase. This increases the inferred quenching pressure for a given dissolved H_2O concentration (Figure 9). Unfortunately the detection limits for measurement of dissolved CO_2 in glasses are typically 30 ppm for the most commonly used analytical techniques (infrared spectroscopy and ion microprobe, Ihinger et al., 1994).

This problem could therefore jeopardise the use of volatile degassing as a useful tool to reconstruct palaeo-ice thicknesses. However, in general subglacially erupted magmas are likely to be almost CO_2 –free (e.g. Dixon et al., 2002), especially those degassed at pressures <5 MPa (~550 m ice), due to the low solubility of CO_2 in silicic melts. To date, only one study has directly addressed the CO_2 problem (Edwards et al., 2009), through the use of a manometric technique to accurately measure trace amounts of CO_2. Other studies have either assumed that all CO_2 has degassed (e.g. Dixon et al., 2002; Schopka et al., 2006) or acknowledged that uncertainty about the CO_2 concentrations prevents precise estimation of ice thicknesses (Hoskuldsson et al., 2006; Stevenson et al., 2009).

Other volatile species may also affect the solubility of water (e.g. Aiuppa et al., 2009), as there are complex interactions between the solubilities of multiple volatile species in silicic melts at different redox conditions (e.g. Behrens and Gaillard, 2006). However the effects are likely to be less strong than that of CO_2 (e.g. Cl has little effect on water solubility in basalt and andesite when present at concentrations of <1.9 wt %, Webster et al. 1999). In addition to modifying the Cl and H_2O solubilities, F can also lower the solidus and liquidus temperatures, lower viscosity and change phase equilibria. Cl can influence fluid exsolution, magma rheology and affect the activity of water and therefore can have many indirect effects on the melt properties (Aiuppa et al., 2009).

4.3. Use of other species

Although progressive degassing of sulphur has been noted in basaltic tuya eruptions (Moore and Calk, 1991) no study to date has used degassing of other species to infer quenching pressures, as the solubility-pressure relationships for other volatile species such as F, Cl and SO_2 are less well known than H_2O and CO_2. As chlorine and fluorine are relatively soluble in silicate melts their degassing predominantly occurs at low pressures; fluorine is generally more soluble than chlorine (Aiuppa et al., 2009). In aluminosilicate melts, the solubility of chlorine is a complex function of pressure and water activity. In anhydrous melts, Cl solubility increases with pressure, where as in water-rich melts Cl solubility tends to decrease with pressure (Webster & De Vivo, 2002). However, the relationships also depend on other factors, including melt composition, oxygen fugacity, other volatile concentrations and temperature (Webster and De Vivo, 2002; Aiuppa et al., 2009). The pressure-solubility relationships for fluorine are not currently well known; fluorine concentrations in bulk glasses may

exceed those in melt inclusions (J. Owen, unpublished data). This enrichment is due to crystallisation within lava bodies, which increases the concentration in the remaining melt (Stecher, 1998).

Despite these problems, as recent research is beginning to place better constraints on the pressure of degassing (e.g. Spilliaert et al., 2006; Edmonds, 2008; Aiuppa et al., 2009) halogen concentrations can potentially be used to track degassing at low pressures during subglacial eruptions. As it has been suggested that fluorine degassing from Icelandic rhyolites only occurs at near-atmospheric pressure in vesicular lavas (Stecher, 1998) low fluorine contents may therefore indicate when magma has reached the ice surface and provide a more sensitive barometer than degassing of water.

5. The interpretation of quenching pressures

The solubility pressure calculated from the measured sample water content provides an estimate of the pressure at which the sample quenched. Early studies have simply assumed that this pressure indicates the weight, and therefore thickness of the overlying ice (e.g. Tuffen, 2001; Dixon et al., 2002), and a plot of volatile content vs. elevation may therefore be expected to fall on a solubility-pressure curve corresponding to a given ice thickness (Fig. 10). However there are two major sources of uncertainty about what the quenching pressure indicates – firstly, what causes the loading in the first place and secondly, whether subglacial pressures are equal to the weight of the overlying ice. Additionally, sample heterogeneity may introduce further uncertainty about the significance of the results.

5.1. Loading by ice, meltwater, firn, snow or rock?

607 During a subglacial eruption magma may quench in direct contact with the overlying
608 ice, or within a body of meltwater, the newly-formed volcanic edifice or the bedrock
609 (Fig. 11a). Therefore the pressure experienced by quenching magma may reflect a
610 combination of loading by ice, meltwater, firn, snow or rock, all of which have
611 different densities. This would lead to contrasting volatile content-elevation
612 relationships, depending upon the density of the loading material (Fig. 11b). To date
613 only two studies (Tuffen and Castro, 2009; Stevenson et al., 2009) have
614 acknowledged this important point. For the most reliable information about ice
615 thicknesses it is therefore preferable to sample from lithofacies that are known to have
616 quenched in direct contact with ice or meltwater. However, in reality this may be
617 difficult.

618 Facies likely to have quenched in contact with ice include lavas with sub-
619 horizontal columnar joints (e.g. Lescinsky and Fink, 2000; Tuffen et al., 2001, Lodge
620 and Lescinsky, 2009) and pillow lavas with steep sides thought to be ice-contact
621 features (Edwards et al., 2009). Fragmental hydroclastic facies such as hyalotuffs are
622 likely to have quenched within a meltwater column (e.g. Guðmundsson, 2003),
623 although large clasts may move significantly within the water column as they cool,
624 creating uncertainty about exactly where quenching occurred. Hyaloclastites
625 generated through quench fragmentation at lava margins (e.g. Tuffen et al., 2001) are
626 likely to have been loaded by overlying deposits when they quenched. The same is
627 true of intrusive lava bodies such as sills and dykes within either bedrock or juvenile
628 volcanic deposits. Quenching in hyaloclastites and intrusive lavas probably therefore
629 occurs at pressures that reflect loading by rock as well as ice or meltwater. Rock
630 density may vary greatly, from 2700 kg m^{-3} for basaltic crust (Hoskuldsson and

631 Sparks, 1997) to ~1900 kg m^{-3} for basaltic hyaloclastites (Schopka et al., 2006) and
632 even lower for vesicular pyroclastic deposits.
633 As the top 40-70 m of temperature glaciers and ice sheets commonly consists
634 of poorly-compacted firn and snow (Paterson, 1994), the mean density of a thin ice
635 sheet/glacier (<150 m) is likely to be substantially lower than the commonly-used ice
636 density of 917 kg m^{-3} (Tuffen and Castro, 2009). A typical firn density is around 700
637 kg m^{-3}. Any ice thickness estimates, especially for thin ice, therefore need to consider
638 depth-dependent density of ice, firn and snow and a mean ice density value of 917 kg
639 m^{-3} may be inappropriate.
640
641 **5.2. Case studies – H_2O degassing at Hrafntinnuhryggur and Helgafell, Iceland.**
642 Tuffen and Castro (2009) reconstructed degassing from the feeder dyke to the surface
643 during a small-volume effusive rhyolitic eruption at Hrafntinnuhryggur, Krafla,
644 Iceland. Lithofacies relationships show that the eruption pierced thin ice (35-75 m),
645 which was likely to have been dominated by firn. Water concentrations were
646 measured using infra-red spectroscopy, for details of the analytical procedure see
647 Tuffen and Castro (2009). As criteria for equilibrium degassing of water-saturated
648 magma are met (vesicles present and an effusive rhyolitic eruption), the glass water
649 content ought to lie close to the pressure-solubility for water in rhyolitic melt.
650 However, when water content is plotted against distance beneath the upper
651 surface of the lava (Fig. 12) it is found to be higher than expected if loading occurred
652 by the weight of firn alone (blue curve). Instead the measured water contents are
653 better fit if bedrock (basaltic hyaloclastite with a density of 1900 kg m^{-3}) also
654 contributed to loading (66 % bedrock and 34 % firn provides the best fit).

Two field observations are consistent with this model: 1) where exposed the feeder dyke cuts basaltic hyaloclastite bedrock, and 2) based on the topography of the area at least 40 m of rock is thought to have been eroded from above the feeder dyke. This study allows detailed investigation of shallow degassing as there are tight constraints on the ice/firn thickness and extra geological information about the extent of post-eruptive erosion. However in many cases this information is lacking, so it may be very difficult to reliably interpret volatile contents when the relative contribution of ice/firn/meltwater and rock to loading is not known.

Intriguingly, Schopka et al. (2006) found little difference in the volatile content of basaltic glasses from shallow intrusions, hyaloclastites and pillow lava selvages at the Pleistocene Helgafell tindar in south-west Iceland. One might expect markedly different quenching pressures due to quenching beneath variable thicknesses of hyaloclastite deposits. One explanation is that only 20-40 m of erosion is thought to have occurred at the tindar summit (based on the geomorphology of the edifice), and potentially less on its flanks where samples were collected. The intrusive deposits may have therefore quenched close to the edifice surface, consistent with their irregular shape. The problem of partial loading by rock will therefore be most important at strongly eroded edifices where many tens or hundreds of metres of overlying rock may have been removed.

5.3. Non-glaciostatic cavity pressures

A major assumption that has underpinned much thinking about the meaning of quenching pressures is that cavity pressures are glaciostatic – in other words, that the pressure of meltwater within subglacial cavities is equal to the weight of the overlying ice (e.g. Paterson, 1994). However, cavity pressure may be considerably less than

680 glaciostatic (underpressure) if there is a hydrological connection established with
681 either the ice surface or the ice margin. If meltwater is moving within an arborescent
682 system of cavities melted upwards into the ice (Nye channels) then underpressure is
683 favoured by high meltwater fluxes, and there is a critical meltwater flux necessary to
684 maintain low pressure conditions (Hooke, 1984).

685 The development of ice cauldrons during subglacial eruptions such as Gjálp is
686 convincing evidence that underpressure can develop (Guðmundsson et al., 2004), as
687 downward deformation of the ice surface is driven by low pressure conditions at the
688 base of the ice (an underpressure of ~2 MPa is consistent with the rate of ice
689 deformation). Low pressure developed due to meltwater drainage into the
690 neighbouring Grímsvötn caldera, rather than due to the negative pressure changes
691 predicted by Hoskuldsson and Sparks (1997) for effusive basaltic eruptions under ice.
692 This is because the heat transfer efficiency was low enough to favour overall volume
693 increase and meltwater drainage from the eruption site (Guðmundsson et al., 2004).

694 There is a growing body of field evidence for localised drainage of meltwater
695 from the eruption site during a variety of different subglacial eruption types spanning
696 basaltic to rhyolitic magmas and from tindars to tuyas (Schopka et al., 2006; Skilling,
697 2009; Tuffen et al., 2001; 2002). Therefore underpressure may be expected to develop
698 during many subglacial eruptions where active meltwater drainage is occurring, and
699 therefore pressure experienced by magma quenching in contact with meltwater may
700 be considerably less than glaciostatic (Fig. 13a).

701 Two papers have discussed the consequences of underpressure for the
702 degassing behaviour of magma and the style of eruptions. Schopka et al. (2006) found
703 that the water content of glasses at Helgafell tindar was significantly lower than that
704 expected from the inferred ice thickness and solubility-pressure relationships. They

noted that the inferred underpressure of 1-2 MPa is similar to the underpressure thought to have developed at Gjálp in 1996, and identified deposits consistent with channelized syn-eruptive meltwater drainage towards the nearby ice margin. Schopka et al. attributed the unusual explosivity of the Helgafell tindar eruption with the low pressure conditions that developed during the eruption.

Hoskuldsson et al. (2006) discovered pillow lavas near Kverkfjoll, Iceland that have remarkably vesicular interiors. The high water content of lava margins is consistent with quenching beneath thick ice (~1 km) but the vesicularity of lava interiors was attributed to a sudden pressure decrease during the emplacement and cooling of the pillow lavas. The authors suggested that meltwater drainage in an [eruption-triggered] jökulhlaup may have been responsible. There is compelling evidence for major volcanically-triggered jökulhlaups in the Kverkfjöll area (Carrivick et al., 2004), supporting this hypothesis.

As non-glaciostatic cavity pressures may commonly develop during subglacial eruptions this is a further factor that may decouple inferred quenching pressures from the actual thickness of overlying ice (Fig. 13b). It will affect only deposits loaded by meltwater when they quench, and so will not be a problem for ice-contact facies.

5.4. Interpreting heterogeneous volatile contents

Figure 14 shows the range of quenching pressures inferred for the heterogeneous welded obsidian breccia at SE Rauðfossafjöll (Fig. 14a, described in section 3.3) and for the variably perlitised rhyolitic lava lobe at Bláhnúkur (Fig. 14b, described in section 3.1), assuming that the water content = total volatiles – 0.6 wt %, Denton et al., 2009). The water contents of the SE Rauðfossafjöll sample, taken from the feeder dyke that fed a subaerial tuya-capping lava flow, are consistent with quenching

730 pressures between 0.14 and 0.69 MPa, equivalent to 6-30 m of overlying lava
731 (assuming a density of 2300 kg m^{-3}). Given the positions of the sampled conduit lava
732 outcrop approximately 25-30 m below the upper carapace of the lava flow it fed, the
733 higher end of these values is therefore more appropriate. The most degassed material
734 was a fine-grained welded breccia formed during fracturing of the lava, which
735 allowed transient degassing to a low confining pressure that is considerably lower
736 than the load of the overlying lava. The data therefore illustrates an important point –
737 that there may be strong spatial variations in the amount of degassing within
738 individual samples due to processes such as brittle-ductile deformation, which means
739 that samples containing heterogeneous magmatic volatiles must be treated with
740 extreme caution.
741 The data for the variably perlitised Bláhnúkur sample (Fig. 14b) indicate how
742 unreasonably high inferred ice thicknesses, due to hydration, can in some cases be
743 readily identified. The range of reasonable ice thicknesses corresponds to the range of
744 ice thicknesses inferred from tuya eruptions in the Bláhnúkur region during the last
745 glacial period (McGarvie et al., 2006). This corresponds well to the inferred ice
746 thickness from the non-hydrated sample, whereas values of close to 2 km are clearly
747 unrealistic. However, if hydration is more subtle or there is no independent supporting
748 evidence for regional thicknesses around the time of the eruption erroneous values
749 may be less readily recognised. The effects of sample hydration are to shift the water
750 content-elevation curve to the right of the "real" values that reflect magma degassing
751 (Fig. 13b).
752
753 **6. The significance of degassing during subglacial eruptions**

In this section we discuss the extent to which magma degassing may control the mechanisms and hazards posed by subglacial eruptions. The potential environmental effects of volcanic gas emissions are also discussed.

6.1. How does magma degassing control eruption mechanisms?

To date we have little understanding of how magma degassing may influence the mechanisms of eruptions under ice. Magmatic volatiles are thought to largely control the mechanism of subaerial silicic eruptions, with explosive "magmatic" activity favoured by the retention of gases and transitions to effusive activity occurring when gases become able to escape from magma during its ascent to the surface (transition from closed to open-system degassing; Eichelberger et al., 1986).

In subglacial silicic eruptions explosively generated deposits are characterised by highly inflated pyroclasts (Tuffen et al., 2002; Stevenson et al., 2009), indicating substantial exsolution of retained magmatic volatiles in the conduit. Deposits indicate the rapid emplacement of pyroclastic debris within substantial well-drained cavities in the ice followed by breaching of the ice surface and possibly a major subaerial explosive phase. The products of non-explosive silicic eruptions are typically less vesicular and there is abundant evidence for emplacement of lavas in close proximity to ice (Tuffen et al., 2001).

It is not currently known whether the explosivity of rhyolitic subglacial eruptions is controlled by volatile degassing. Current models suggest that the explosive-effusive transition may be linked to the eruption rate, as this controls the amount of space above growing volcanic edifices in which meltwater can collect and interact explosively with magma (Tuffen et al., 2007; Tuffen 2007). If this is the case, the important question is then what controls the eruption rate; magmatic volatiles are

779 likely to play a major role (e.g. Wilson, 1980). It is plausible that explosive eruptions
780 are indeed those with high eruption rates, high magmatic volatile contents and
781 therefore high magma vesicularity, but this has not been proven. Perhaps counter-
782 intuitively, recent experiments have shown that explosive rhyolite-water interaction is
783 favoured by degassed, high-viscosity melt, as brittle melt fragmentation may create
784 the surface area needed to initiate runaway fuel-coolant interactions (Austin-Erickson
785 et al., 2008). If this were the case for subglacial eruptions phreatomagmatic tephra
786 formed in violent explosions could be expected to be relatively vesicle-poor.
787 However, this is instead found in non-explosively generated deposits. Clearly more
788 research is needed to investigate links between the explosivity of subglacial eruptions
789 and the degree of magma vesiculation.

790 What controls the style of subglacial basaltic eruptions may be an even more
791 complex problem, as the explosivity of basaltic eruptions is largely determined by the
792 extent and violence of interaction with external water (Wohletz, 1986). In some
793 instances volatile exsolution may also be important in triggering "magmatic"
794 fragmentation (Cervantes and Wallace, 2003; Houghton and Gonnermann, 2008).
795 Changes in shallow degassing and vesiculation at individual vents over short
796 timescales may lead to rapid shifts in the style of activity (Houghton et al., 1999;
797 Cervantes and Wallace, 2003). As is the case for silicic eruptions, it is not obvious
798 how shallow degassing affects the explosivity of basalt-water interactions. However,
799 it is believed that the style of eruptions within ice-confined meltwater lakes becomes
800 increasingly explosive when the water depth is less than 200 m deep, which
801 corresponds to a pressure of less than 2 MPa (summarised in Tuffen, 2007). In some
802 localities this inferred water depth marks the transition from quench hyaloclastites to
803 vesicular hyalotuffs (e.g. Jones, 1969; 1970) and thus a pressure threshold below

804 which substantial magma vesiculation occurs. However, in other localities explosive
805 magma-water interactions may take place at considerably higher confining pressures
806 (Guðmundsson et al., 2004); non-explosive magma-water interaction in submarine
807 and sublacustrine settings may also occur beneath water only metres to tens of metres
808 deep, leading to the formation of pillows (Batiza and White, 2000). How confining
809 pressure controls the explosivity of magma-water interaction and what role
810 vesiculation plays in modifying interaction mechanisms therefore remain poorly
811 understood questions. Detailed studies of the links between multi-species degassing,
812 vesiculation and fragmentation mechanisms during subglacial eruptions are needed to
813 improve our knowledge.
814

815 **7. Conclusions and challenges for future research**

816 Although we are beginning to gain limited understanding of the behaviour of
817 magmatic volatiles during subglacial eruptions there remain many substantial and
818 fundamental gaps in our knowledge that can be filled by future research.
819 – The use of volatile degassing to reconstruct palaeo-ice thicknesses is still in its
820 infancy. Many factors need to be considered before making confident estimates of
821 palaeo-ice thicknesses, including non-equilibrium degassing, hydration, sample
822 heterogeneity, post-quenching sample movement, loading by rock as well as ice and
823 non-glaciostatic pressure in subglacial cavities. Studies of deposits with good
824 secondary constraints on ice thickness (from direct observations of recent eruptions or
825 other geological evidence for ancient eruptions) are first required in order to assess the
826 reliability of using volatile degassing alone.
827 – Detailed studies of the dissolved concentration of a broad range of volatile species
828 (H_2O, CO_2, SO_2, F and Cl) in suites of samples from a variety of subglacial eruption

types are required to better understand multi-species degassing and to what extent it can be used to reconstruct quenching pressures and thus palaeo-ice thicknesses. Particular attention should be paid to previously-ignored species such as F and Cl as they may shed new light on the pressures of shallow degassing.

– More evidence for non-glaciostatic pressures and abrupt changes in pressure during subglacial eruptions needs to be gathered from detailed measurements of volatile concentrations and combined with geological evidence for changes in subglacial meltwater drainage. The effects of pressure changes on the mechanisms of eruptions need to be better understood.

– The analytical techniques used to measure volatile concentrations need to improve on the common practise of using infra-spectroscopy alone to determine H_2O contents in one part of a sample. Multiple analyses are required to quantify the degree of heterogeneity within samples and techniques such as manometry, ion microprobe or electron microprobe are required to analyse other species (CO_2, S, F, Cl).

– There is currently no data tracking magma degassing from the chamber to the surface during subglacial eruptions of any composition. Therefore it is not known how initial volatile contents and subsequent degassing during magma ascent affect eruption mechanisms and associated hazards. Furthermore, calculations of the volatile flux to the environment from subglacial eruptions are yet to be carried out.

– It is not well established whether volatile degassing influences the explosivity of magma-meltwater interactions during subglacial eruptions. Comparison of vesiculation, degassing and fragmentation behaviour during basaltic and rhyolitic eruptions is therefore required.

Acknowledgements

HT was supported by a NERC Research Fellowship and JO by a NERC research studentship. HT and JO were also partly supported by NERC grant NE/G000654/1. JSD received support from the Timothy Jefferson Fund by the Geological Society of London. Thanks to Jennie Gilbert, Harry Pinkerton, Isobel Sides, Marie Edmonds, John Stevenson, Jon Castro and Dave McGarvie for interesting discussions and an anonymous referee for helpful and constructive comments. We are also grateful to Chiara Petrone for assistance with electron microprobe analysis and Richard Brooker for assistance with the FTIR measurements at the University of Bristol.

References

Aiuppa A., Baker D.R., Webster J.R. (2009) Halogens in volcanic systems. Chemical Geology 263: 1–18.

Austin-Erickson, A., Buttner, R., Dellino, P., 2008. Phreatomagmatic explosions of rhyolitic magma: Experimental and field evidence. J. Geophys. Res., 113, art. no. B11201.

Batiza, R., White, J.D.L., 2000. Submarine lava and hyaloclastite. In: H. Sigurdsson (Editor), Encyclopaedia of Volcanoes. Academic Press, San Diego, pp. 361–382.

Behrens, H., Gaillard, F., 2006. Geochemical aspects of melts: Volatiles and redox behaviour. Elements 2: 275-280.

878 Blank, J.G, Brooker, R.A., 1994. Experimental studies of carbon dioxide in silicate
879 melts: solubility, speciation, and stable carbon isotope behaviour. Rev. Min.
880 Geochem. 30: 157–186.
881
882 Carroll, M.R, Webster, J.D., 1994. Solubilities of sulfur, noble gases, chlorine and
883 fluorine in magmas. Rev. Min. Geochem. 30: 231–279.
884
885 Carrivick, J.L., Russell, A.J., Tweed, F.S., 2004. Geomorphological evidence for
886 jökulhlaups from Kverkfjöll volcano, Iceland. Geomorphology 63: 81-102.
887
888 Castro, J.M., Manga, M., Martin, M.C., 2005. Vesiculation rates of obsidian domes
889 inferred from H_2O concentration profiles. Geophys. Res. Lett. 32, art. no. L21307.
890
891 Castro, J.M., Beck, P., Tuffen, H., Nichols, A., Dingwell, D.B., 2008. Timescales of
892 spherulite crystallization in obsidian inferred from water concentration profiles. Am.
893 Mineral. 93: 1816–1822.
894
895 Castro, J.M., Gardner, J.E., 2008. Did magma ascent rate control the explosive-
896 effusive transition at the Inyo volcanic chain, California? Geology 36: 279-282.
897
898 Cervantes, P., Wallace, P., 2003. Magma degassing and basaltic eruption styles: a
899 case study of similar to 2000 year BP Xitle volcano in central Mexico. J. Volcanol.
900 Geotherm. Res. 120: 249-270.
901

902 DeGroat-Nelson, P.J., Cameron, B.I., Fink, J.H., Holloway, J.R., 2001. Hydrogen
903 isotope analysis of rehydrated silicic lavas: implications for eruption mechanisms.
904 Earth Planet. Sci. Lett. 185: 331-341.
905
906 Denton, J.S., Tuffen, H., Gilbert, J.S., Odling, N., 2009. The hydration and alteration
907 of perlite and rhyolite. J. Geol. Soc. Lond. 166: 895-904.
908
909 Dixon, J.E., Stolper, E.M., Delaney, J.R., 1988. Infrared spectroscopic measurements
910 of CO_2 and H_2O in Juan de Fuca Ridge basaltic glasses. Earth Planet. Sci.
911 Lett. 90: 87–104.
912
913 Dixon, J.E., Stolper, E.M., 1995. An experimental study of water and carbon dioxide
914 solubilities in mid-ocean ridge basaltic liquids. Part II: Applications to degassing. J.
915 Petrol. 36: 1633-1646.
916
917 Dixon, J.E., Clague, D.E., Wallace, P., Poreda, R., 1997. Volatiles in alkalic basalts
918 from the North Arch volcanic field, Hawaii: Extensive degassing of deep submarine-
919 erupted alkalic series lavas. J. Petrol. 38: 911-939.
920
921 Dixon, J.E., Filiberto, J.R., Moore, J.G., Hickson, C.J., 2002. Volatiles in basaltic
922 glasses from a subglacial volcano in northern British Columbia (Canada):
923 implications for ice sheet thickness and mantle volatiles. In: Smellie, J.L., Chapman,
924 M.G. (Editors), Volcano–ice Interaction on Earth and Mars. Spec. Pub. Geol. Soc.
925 Lond. 202, pp. 255–271.
926

927 Edmonds, M., 2008. New geochemical insights into volcanic degassing. Phil. Trans.
928 Roy. Soc. A 366: 4559-4579.
929
930 Edwards, B.R., Skilling, I.P., Cameron, B., Haynes, C., Lloyd, A., Hungerford,
931 J.H.D., 2009. Evolution of an englacial volcanic ridge: Pillow Ridge tindar, Mount
932 Edziza volcanic complex, NCVP, British Columbia, Canada. J. Volcanol. Geotherm.
933 Res. 185: 251-275.
934
935 Eichelberger, J.C., Carrigan, C.R., Westrich, H.R., Price, R.H., 1986. Non-explosive
936 silicic volcanism. Nature 323: 598-602.
937
938 Fine, G., Stolper, E., 1986. Dissolved carbon-dioxide in basaltic glasses -
939 concentrations and speciation. Earth Planet. Sci. Lett. 76: 263-278.
940
941 Gíslason S.R., Snorrason, Á., Kristmannsdóttir, H.K., Sveinbjörnsdóttir Á.E.,
942 Torsander, P., Ólafsson, J., Castet, S., Dupré, B., 2002. Effects of volcanic eruptions
943 on the CO_2 content of the atmosphere and the oceans: the 1996 eruption and flood
944 within the Vatnajökull Glacier, Iceland. Chem. Geol. 190: 181-205.
945
946 Guðmundsson, M.T., Sigmundsson, F., Björnsson, H., Högnadóttir, Þ., 2004. The
947 1996 eruption at Gjálp, Vatnajökull ice cap, Iceland: Course of events, efficiency of
948 heat transfer, ice deformation and subglacial water pressure. Bull. Volcanol. 66: 46-
949 65.
950

951 Guðmundsson, M.T., 2003. Melting of ice by magma–ice–water interactions during
952 subglacial eruptions as an indicator of heat transfer in subaqueous eruptions. In:
953 White, J.D.L., Smellie, J.L., Clague, D. (eds) Explosive subaqueous volcanism. Am
954 Geophys. Union Mon. 140, pp. 61–72.
955
956 Hooke, R.L., 1984. On the role of mechanical energy in maintaining subglacial water
957 conduits at atmospheric pressure. J. Glaciol. 30: 180-187.
958
959 Höskuldsson, A., Sparks, R.S.J., 1997. Thermodynamics and fluid dynamics of
960 effusive subglacial eruptions. Bull. Volcanol. 59: 219-230.
961
962 Höskuldsson, A., Sparks, R.S.J., Carroll M.R., 2006. Constraints on the dynamics of
963 subglacial basalt eruptions from geological and geochemical observations at
964 Kverkfjöll, NE-Iceland. Bull. Volcanol. 68: 689-701.
965
966 Houghton, B.F., Gonnermann, H.M., 2008. Basaltic explosive volcanism: Constraints
967 from deposits and models. Chemie der Erde 68: 117-140.
968
969 Humphreys, M.C.S., Menand, T., Blundy, J.D., Klimm, K., 2008. Magma ascent rates
970 in explosive eruptions: Constraints from H_2O diffusion in melt inclusions. Earth
971 Planet. Sci. Lett. 270: 25-40.
972
973 Huybers, P., Langmuir, C., 2009. Feedback between deglaciation, volcanism, and
974 atmospheric CO_2. Earth Planet. Sci. Lett. 286: 479-491.
975

976 Ihinger, P.D., Hervig, R.L., McMillan, P.F., 1994. Analytical methods for volatiles in
977 glasses. Rev. Min. Geochem. 30: 67–121.
978
979 Jakobsson, S.P., 1978. Environmental factors controlling the palagonitization of the
980 Surtsey tephra, Iceland. Bull. Geol. Soc. Den. 27: 91-105.
981
982 Jarosch, A., Gudmundsson, M.T., Hognadottir, T., Axelsson, G., 2008. Progressive
983 cooling of the hyaloclastite ridge at Gjálp, Iceland, 1996-2005. J. Volcanol.
984 Geotherm. Res. 170: 218-229.
985
986 Johnson, M.C., Anderson, A.T., Rutherford, M.J., 1994. Pre-eruptive volatile contents
987 of magmas. Rev. Min. Geochem. 30: 281-330.
988
989 Jones, J.G., 1969. Intraglacial volcanoes of the Laugarvatn region, south–west Iceland
990 I. Quart. J. Geol. Soc. Lond. 124: 197–211.
991
992 Jones, J.G., 1970. Intraglacial volcanoes of the Laugarvatn region, southwest Iceland,
993 II. J. Geol., 78: 127-140.
994
995 Liu, Y., Zhang, Y.X., Behrens, H., 2005. Solubility of H_2O in rhyolitic melts at low
996 pressures and a new empirical model for mixed H_2O-CO_2 solubility in rhyolitic melts.
997 J. Volcanol. Geotherm. Res. 143: 219-235.
998

McGarvie, D.W., Stevenson, J.A., Burgess, R., Tuffen, H., Tindle, A., 2007. Volcano–ice interactions at Prestahnúkur, Iceland: rhyolite eruption during the last interglacial–glacial transition. Ann. Glaciol. 45: 38–47.

Maclennan, J., Jull, M., McKenzie, D.P., Slater, L., Gronvold, K., 2002. The link between volcanism and deglaciation in Iceland. Geochem. Geophys. Geosyst. doi:10.1029/2001GC000282.

McMillan, P.F., 1994. Water solubility and speciation models. Rev. Min. Geochem. 30: 131–156.

Mastin, L.G., Christiansen, R.L., Thornber, C., Lowenstern, J., Beeson, M., 2004. What makes hydromagmatic eruptions violent? Some insights from the Keanakakoi Ash, Kilauea Volcano, Hawaii. J. Volcanol. Geotherm. Res. 137: 15–31.

Moore, J.G., 1970. Water content of basalt erupted on the ocean floor. Contrib. Mineral. Petrol. 28: 272-279.

Moore, J.G., Calk, L., 1991. Degassing and differentiation in subglacial volcanoes, Iceland. J. Volcanol. Geotherm. Res. 46: 157–180.

Moore, J.G., Hickson, C.J., Calk, L., 1995. Tholeiitic–alkalic transition at subglacial volcanoes, Tuya region, British Columbia. J. Geophys. Res. 100: 24,577–24,592.

1024 Moore, J.G., Vennemann, T., Carmichael, I.S.E., 1998. An empirical model for the
1025 solubility of H_2O in magmas to 3 kilobars. Am. Mineral. 83: 36-42.
1026
1027 Newman, S., Stolper, E.M., Epstein, S., 1986. Measurement of water in rhyolitic
1028 glasses: calibration of an infrared spectroscopic technique. Am. Mineral. 71: 1527-
1029 1541.
1030
1031 Newman, S., Epstein, S., Stolper, E., 1988. Water, carbon dioxide, and hydrogen
1032 isotopes in glasses from the ca. 1340 A. D. eruption of the Mono Craters, California:
1033 Constraints on degassing phenomena and initial volatile content. J. Volcanol.
1034 Geotherm. Res. 35: 75-96.
1035
1036 Newman, S., Lowenstern, J.B., 2002. VolatileCalc: a silicate melt-H2O–CO2 solution
1037 model written in Visual Basic. Comp. Geosci. 28: 597–604.
1038
1039 Nichols, A.R.L., Carroll, M.R., Höskuldsson, A., 2002. Is the Iceland hot spot also
1040 wet? Evidence from the water contents of undegassed submarine and subglacial
1041 pillow lavas. Earth Planet. Sci. Lett. 202: 77–87.
1042
1043 Pagli, C., Sigmundsson, F., 2008. Will present day glacier retreat increase volcanic
1044 activity? Stress induced by recent glacier retreat and its effect on magmatism at the
1045 Vatnajökull ice cap, Iceland. Geophys. Res. Lett. 35: art. no. L09304.
1046
1047 Papale, P., Moretti, R., Barbato, D., 2006. The compositional dependence of the
1048 saturation surface of H_2O+CO_2 fluids in silicate melts. Chem. Geol. 229: 78-95.

Paterson, W.S.B., 1994. The Physics of Glaciers, 3rd ed. Pergamon Press, Oxford. 480 pp.

Proussevitch, A.A., Sahagian, D.L., 1996. Dynamics of coupled diffusive and decompressive bubble growth prior to volcanic eruption. J. Geophys. Res. 101: 17447–17456.

Rust, A.C., Cashman, K.V., 2007. Multiple origins of obsidian pyroclasts and implications for changes in the dynamics of the 1300 BP eruption of Newberry Volcano, USA. Bull. Volcanol. 69: 825-845.

Schopka, H.H., Guðmundsson, M.T., Tuffen, H., 2006. The formation of Helgafell, SW-Iceland, a monogenetic subglacial hyaloclastite ridge: Sedimentology, hydrology and ice-volcano interaction. J. Volcanol. Geophys. Res. 152: 359-377.

Skilling, I.P., 1994. Evolution of an englacial volcano: Brown Bluff, Antarctica. Bull. Volcanol. 56: 573-591.

Skilling, I.P., 2009. Subglacial to emergent basaltic volcanism at Hlöðufell, south-west Iceland: A history of ice-confinement. J. Volcanol. Geotherm. Res. 185, 276-289.

Simons, K., Dixon, J., Schilling, J.G., Kingsley, R., Poreda, R., 2002. Volatiles in basaltic glasses from the Easter-Salas y Gomez Seamount Chain and Easter

1074 Microplate: Implications for geochemical cycling of volatile elements. Geochem.
1075 Geophys. Geosyst. 3: art. no. 1039, doi: 10.1029/2001GC000173.
1076
1077 Smellie, J.L., 2000. Subglacial eruptions. In: H. Sigurdsson (Editor), Encyclopaedia
1078 of Volcanoes. Academic Press, San Diego, pp. 403-418.
1079
1080 Smellie, J.L., 2008. Basaltic subglacial sheet-like sequences: evidence for two types
1081 with different implications for the inferred thickness of associated ice. Earth Sci. Rev.
1082 88: 60-88.
1083
1084 Smellie, J.L., Johnson, J.S., McIntosh, W.C., Esserb, R., Gudmundsson, M.T.,
1085 Hambrey, M.J., van Wyk de Vries, B., 2008. Six million years of glacial history
1086 recorded in volcanic lithofacies of the James Ross Island Volcanic Group, Antarctic
1087 Peninsula. Palaeogeog. Palaeoclim. Palaeoecol. 260: 122-148.
1088
1089 Smith, J.V., Miyake, Y., Oikawa T., 2001. Interpretation of porosity in dacite lava
1090 domes as ductile- brittle failure textures. J. Volcanol. Geotherm. Res. 112: 25-35.
1091
1092 Sparks, R.S.J., 2003. Dynamics of magma degassing. In Oppenheimer C., Pyle, D.M.,
1093 Barclay, J. (eds), Volcanic degassing. Geol. Soc. Lond. Spec. Pub. 213: 5-22.
1094
1095 Spilliaert, N., Metrich, N., Allard, P., 2006. S-Cl-F degassing pattern of water-rich
1096 alkali basalt: Modelling and relationship with eruption styles at Mount Etna volcano.
1097 Earth Plan. Sci. Lett. 248: 772-786.
1098

1099 Stecher, O., 1998. Fluorine geochemistry in volcanic rock series: Examples from
1100 Iceland and Jan Mayen. Geochem. Cosmochim. Acta 62: 3117-3130.
1101
1102 Stevenson, J.A., Smellie, J.S., McGarvie, D., Gilbert, J.S., Cameron, B., 2009.
1103 Subglacial intermediate volcanism at Kerlingarfjöll, Iceland: magma-water
1104 interactions beneath thick ice. J. Volcanol. Geotherm. Res. 185: 337-351.
1105
1106 Stolper, E., Holloway, J.R, 1988. Experimental determination of the solubility of
1107 carbon-dioxide in molten basalt at low-pressure. Earth Planet. Sci. Lett. 87: 397-408.
1108
1109 Tuffen H (2001) Subglacial rhyolite volcanism at Torfajökull, Iceland. PhD thesis,
1110 Open University, Milton Keynes, UK, 381 pp.
1111
1112 Tuffen, H., 2007. Models of ice melting and edifice growth at the onset of subglacial
1113 basaltic eruptions. J. Geophys. Res. 112, art. no. B03203, doi:10.1029/
1114 2006JB004523.
1115
1116 Tuffen, H., Castro, J.M., 2009. An obsidian dyke erupted through thin ice:
1117 Hrafntinnuhryggur, Krafla, Iceland. J. Volcanol. Geotherm. Res. 185: 352–366.
1118
1119 Tuffen, H., Dingwell, D.B., 2005. Fault textures in volcanic conduits: evidence for
1120 seismic trigger mechanisms during silicic eruptions. Bull. Volcanol. 67: 370–387.
1121
1122 Tuffen, H., Gilbert J.S., McGarvie, D.W., 2007. Will subglacial rhyolite eruptions be
1123 explosive or intrusive? Some insights from analytical models. Ann. Glaciol. 45: 87-

94.

Tuffen, H., Gilbert, J.S., McGarvie, D.W., 2001. Products of an effusive subglacial rhyolite eruption: Bláhnúkur, Torfajökull, Iceland. Bull. Volcanol. 63: 179–190.

Tuffen, H., McGarvie, D.W., Pinkerton, H., Gilbert, J.S., Brooker R., 2008. An explosive-intrusive subglacial rhyolite eruption at Dalakvísl, Torfajökull, Iceland. Bull. Volcanol. 70: 841–860, DOI:10.1007/s00445-007-0174-x.

Tuffen, H., McGarvie, D.W., Gilbert, J.S., Pinkerton, H., 2002b. Physical volcanology of a subglacial-to-emergent rhyolitic tuya at Rauðufossafjöll, Torfajökull, Iceland. In: Smellie, J.L., Chapman, M.G., (Editors) Volcano–ice interaction on Earth and Mars. Geol. Soc. Lond. Spec. Pub. 202, pp. 213–236.

Tuffen, H., Pinkerton, H., Gilbert, J.S., McGarvie, D.W., 2002a. Melting of the glacier base during a small-volume subglacial rhyolite eruption: evidence from Bláhnúkur, Iceland. Sediment. Geol. 149: 183–198.

Webster, J.D., Kinzler, R.J., Mathez, E.A., 1999. Chloride and water solubility in basalt and andesite melts and implications for magmatic degassing. Geochim. Cosmochim. Acta 63: 729-738.

Webster, J.D., De Vivo, B., 2002. Experimental and modeled solubilities of chlorine in aluminosilicate melts, consequences of magma evolution, and implications for

exsolution of hydrous chloride melt at Mt. Somma-Vesuvius. Am. Mineral. 87: 1046–1061.

Westrich, H.R., Eichelberger, J.C., 1994. Gas transport and bubble collapse in rhyolitic magma: an experimental approach. Bull. Volcanol. 56: 447–458.

Wilson, L., 1980. Relationships between pressure, volatile content and ejecta velocity in three types of volcanic explosion. J. Volcanol. Geophys. Res. 8: 297-313.

Wohletz, K.H., 1986. Explosive magma-water interactions: Thermodynamics, explosion mechanisms, and field studies. Bull. Volcanol. 48: 245-264.

Wright, I.C., Gamble, J.A., Shane, P.A.R., 2003. Submarine silicic volcanism of the Healy caldera, southern Kermadec arc (SW Pacific): I - volcanology and eruption mechanisms. Bull. Volcanol. 65: 15-29.

Zhang, Y.X., 1999. H_2O in rhyolitic glasses and melts: measurement, speciation, solubility, and diffusion. Rev. Geophys. 37: 493–516.

Figure captions

Figure 1. Schematic cartoon showing magma degassing from the chamber to the surface during a basaltic tuya eruption through ice hundreds of metres thick. In turn low-vesicularity pillows, low-vesicularity quench hyaloclastite, vesicular hyalotuffs and degassed subaerial lavas are emplaced. Initial volatile contents are recorded by trapping of melt inclusions within phenocrysts growing in the chamber and magma progressively vesiculates as it rises to the surface.

Figure 2. (a) A glassy pillow margin from Helgafell, south-west Iceland (Schopka et al., 2006), showing a small proportion of rounded vesicles indicative of bubble growth in volatile saturated magma. Polished wafer for infra-red spectroscopic analysis, photographed in plane-polarised light. **(b)** Cartoon showing rise of rhyolitic magma within a dyke of width 2h. Other symbols are defined in the text.

Figure 3. (a) Cartoon illustrating how lava may degas at the vent to a lower confining pressure before flowing downslope to higher pressure conditions beneath thicker ice. This process may create volatile-poor lavas degassed to near-atmospheric pressure that are found near the base of substantial subglacially erupted edifices. **(b)** An ice-confined rhyolitic lava at Bláhnúkur, Iceland that has flowed ~100 m downslope from its feeder dyke at the top of the edifice. **(c)** Cartoon illustrating how clasts may move during hydromagmatic activity within an ice-confined meltwater lake. Significant movement may occur during quenching, especially if explosive magma-water interactions occur in a substantial depth of meltwater. Clast movement during

deposition is also inevitable and may transport clasts an appreciable vertical distance beneath the zone of quenching.

Figure 4. The relationship between the total volatile content of variably hydrated subglacially erupted rhyolitic glasses from Torfajökull, Iceland and the temperature of fastest weight loss during bulk extraction experiments (using the thermogravimetric technique), from Denton et al. (2009). As hydrated water is predominant in molecular form and loosely bound to the glass it is lost at lower temperatures than more tightly-bound magmatic water (mostly OH^-). Therefore the behaviour of samples during dehydration experiments may help to indicate which are hydrated.

Figure 5. (a) and **(b)** The margin of a subglacially erupted rhyolitic lava lobe at Bláhnúkur, Iceland showing strong gradient in the degree of perlitisation, with pale grey perlitised obsidian at the lobe edge giving way to non-hydrated black obsidian in the lava interior. **(c)** The total volatile contents (predominantly H_2O) of samples from the four textural zones indicated in (a) and (b), showing much higher values for more-perlitic lava at the lobe edge than less-perlitised lava further towards the lava interior.

Figure 6. (a) A strong gradient in water content across a perlitic bead in hydrated subglacially erupted rhyolitic obsidian sample gge from Bláhnúkur, Iceland as measured by infra-red spectroscopy. The increase in intensity of the 3550 cm-1 OH_T and 1630 cm^{-1} H_2O_m peaks as the bead margin is approached indicates water enrichment by hydration. **(b)** The traverse measured in (a), showing a typical ~400 μm wide perlitic bead defined by dark cracks. **(c)** The total glass water content across the measured profile, showing strong enrichment towards the bead margin.

Figure 7. A water content map determined using infra-red spectroscopy (at the University of Bristol) on a sample of rhyolitic obsidian from the upper part SE Raudfossafjoll tuya, Iceland. There is considerable heterogeneity over scales of hundreds of microns to millimetres associated with the presence of welded fragmental material (tuffisites) formed during fracture and healing of the magma. Modified from Tuffen (2001).

Figure 8. A sample of subglacially erupted rhyolitic obsidian from Bláhnúkur, Iceland with highly heterogeneous fluorine content. Five different coloured flow bands were analysed (Table 3) and each has distinctive fluorine contents (individual data points are plotted as crosses over each corresponding band, average values for each band are also shown as other shapes). This heterogeneity may reflect shallow mixing of distinct magma batches or contrasting vesiculation and degassing paths of bands of neighbouring melt.

Figure 9. Pressure-solubility relationships for H_2O in basalts and rhyolites at different magma temperatures and CO_2 contents, calculated using VolatileCalc (Newman and Lowenstern, 2002). **(a)** Basaltic magma, where the CO_2 content has an extremely strong effect on quenching pressures and inferred ice thicknesses, especially at low H_2O concentrations. However, as discussed in the text, it is highly unlikely that water-poor magmas will contain this quantity of CO_2. According to the VolatileCalc software, magma temperature does not strongly affect water solubility in basalt, the 1150 °C curves correspond with those at 1250 °C. **(b)** Rhyolitic magma, where the inferred quenching pressure and ice thickness depends strongly on the CO_2 content,

with only 30 ppm of CO_2 (the detection limit for most analytical techniques) greatly increasing the solubility pressure. Magma temperature has only a minor influence on the pressure-solubility relationships.

Figure 10. An example of possible water content-sample elevation relationships for a basaltic eruption with 0 ppm CO_2 and loading by ice with a mean density of 917 kg m^{-3}. The solubility curves for three different ice thicknesses are indicated (330, 500 and 800 m). Plotting sample water contents against their elevations may there indicate the approximate ice thickness, if other factors do not affect the sample volatile contents or quenching pressures. Modified from Schopka et al. (2006).

Figure 11. (a) Cartoon illustrating five different loading scenarios occurring when a subglacial sample is quenched. (1) Quenching at the magma-ice interface, loading by ice + firn. (2) Quenching within juvenile deposits, loading by juvenile deposits + ice + firn. (3) Quenching in direct contact with firn, loading by firn only. (4) Quenching within juvenile deposits, loading by juvenile deposits + meltwater. (5) Quenching within meltwater, loading by meltwater only. In each case the mean density of the overlying material will be different. **(b)** Graph of predicted degassing trends with elevation for a basaltic edifice emplaced beneath 800 m of ice/firn or rock. The different densities of loading materials produce drastic differences in the predicted degassing trends, which would make accurate estimation of ice thicknesses impossible. It is therefore essential to have good constraints on the relative contribution of rock to ice/firn to loading. Curves are labelled with densities (kg m^{-3}) for each loading material.

Figure 12. Magma degassing from the feeder dyke to the surface at Hrafntinnuhryggur, Iceland as shown by decreasing glass water contents with elevation (Tuffen and Castro, 2009). The heterogeneity in water contents at a shallow level (in the subaerial lava carapace) is due to crystallisation within the lava (Castro et al., 2008). Feeder dyke water contents are not consistent with loading by the inferred thickness of firn (~50 m), nor by bedrock alone, but instead by a combination of firn and bedrock (green line). This result is consistent with field evidence for erosion of bedrock from around the feeder dyke (Tuffen and Castro, 2009).

Figure 13. (a) Cartoon illustrating the difference between the piezometric water head (the height to which meltwater would rise within a vertical borehole, which is proportional to the water pressure) and the meltwater head if pressure were glaciostatic. This difference is the underpressure, it has developed here as there is hydrological connection between the vent area and the ice margin. The gradient of the piezometric water head drives meltwater flow, in this case away from the eruption site and towards the ice margin. Modified from Schopka et al., 2006. **(b)** A theoretical dataset showing three different scenarios when glass water content is plotted against elevation at a subglacially erupted edifice. The solid curve shows the expected relationship between quenching pressure and elevation, using a given ice surface elevation consistent with other observations. The green points indicate glaciostatic pressure conditions and data fit well to the modelled curve. Points that plot significantly to the left (red series, lower than expected water content) may indicate underpressured cavity conditions (Schopka et al., 2006). Points that plot far to the right (blue series) may indicate hydration by meteoric water (Denton et al., 2009).

Figure 14. Diagrams illustrating the implications of sample volatile heterogeneity for interpreting quenching pressures. Solubility calculations assume CO_2-free melt and were made using VolatileCalc. **(a)** Heterogeneous water contents in welded lava sample TCO7 from SE Rauðfossafjöll, which was overlain by a subaerial rhyolite lava flow, and their saturation pressures. The grey box illustrates the estimated confining pressure due to the overlying lava. Water contents compatible with lower pressures than this probably reflect degassing to near-atmospheric pressure during fracturing of the lava. This process superimposed melt with contrasting degassing histories within a single welded sample. **(b)** Heterogeneous water contents in a variably perlitised obsidian sample from Bláhnúkur with their saturation pressures and equivalent ice thicknesses indicated.

Figure 15. The possible consequences of a decrease in the level of a meltwater lake during a subglacial eruption. **(a)** Pre-drainage, pillow lavas are being erupted at high water pressure. **(b)** Due to subglacial meltwater drainage the lake level dramatically drops, triggering increased magma vesiculation and explosive interactions with meltwater. Any pillows that have not quenched may vesiculate due to the compression (Hoskuldsson et al., 2006).

1309 FIGURES
1310
1311 Fig. 1
1312
1313

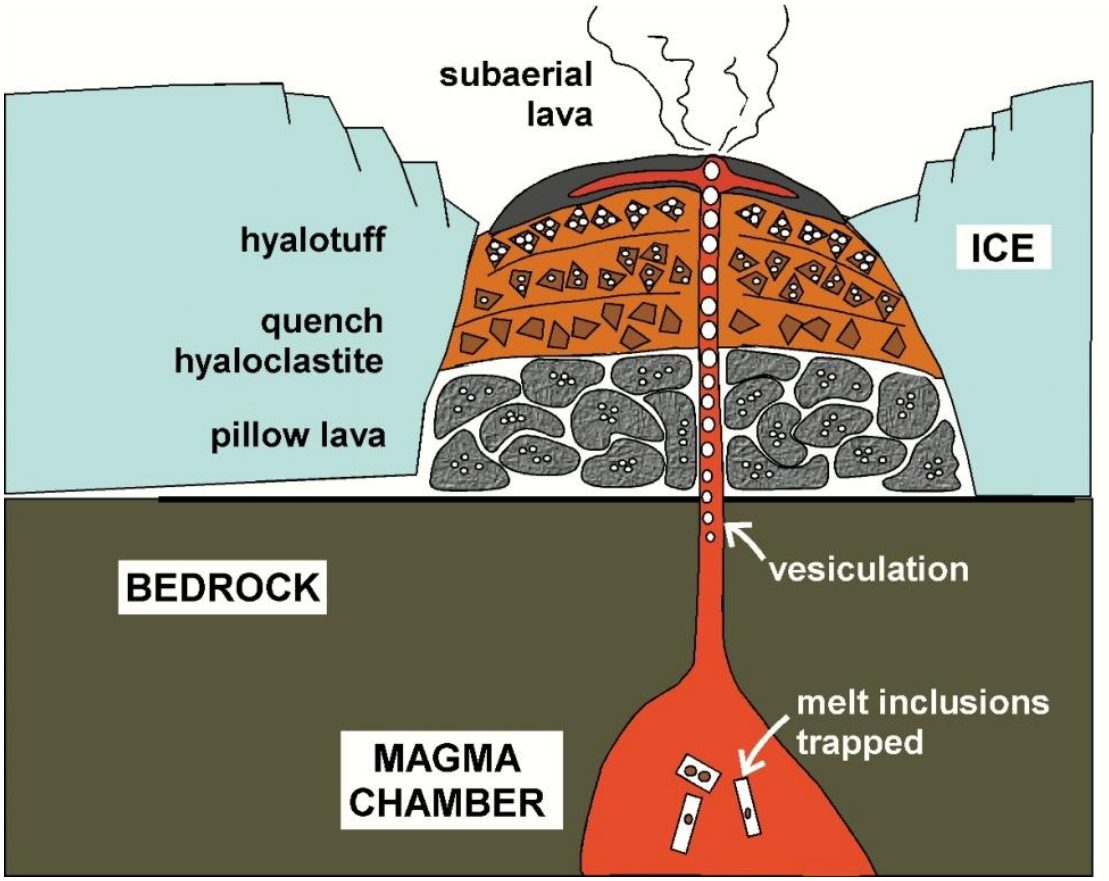

1314

Fig. 2

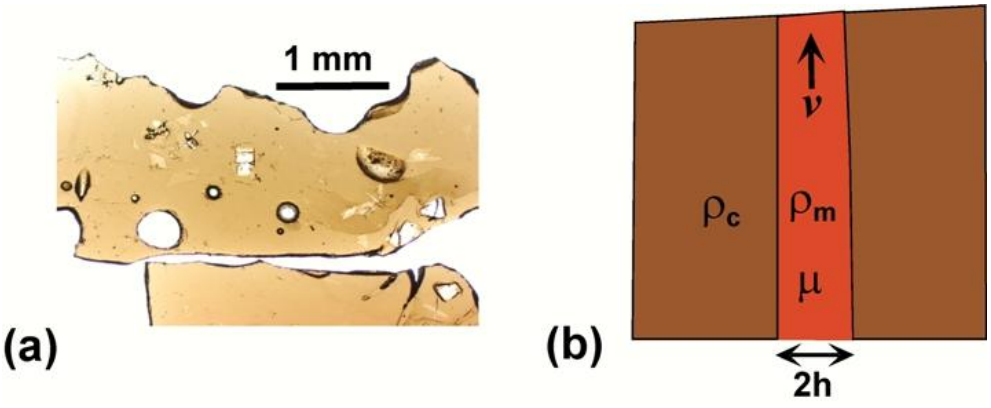

1320
1321 Fig. 3
1322
1323
1324

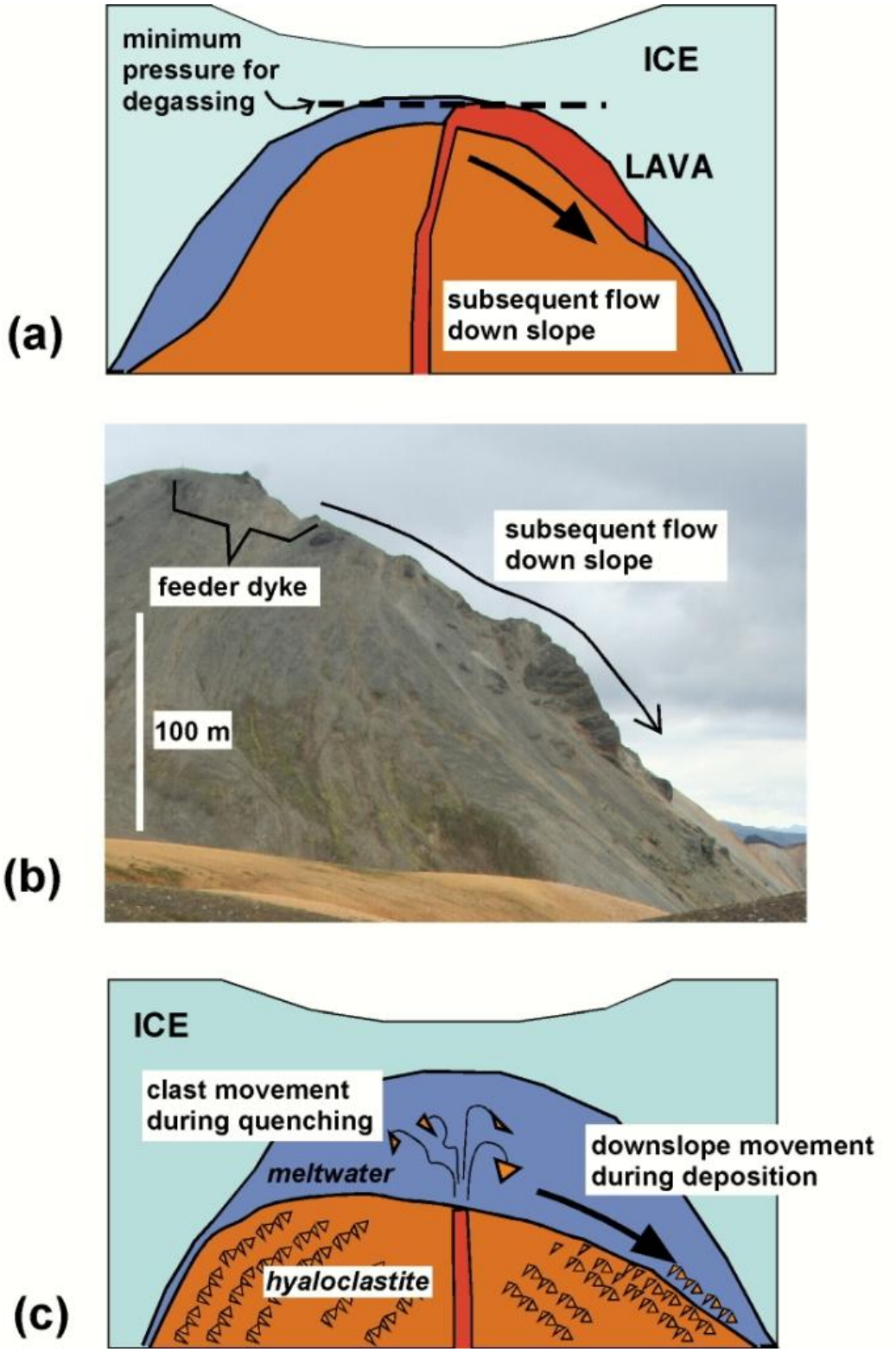

1325 Fig. 4

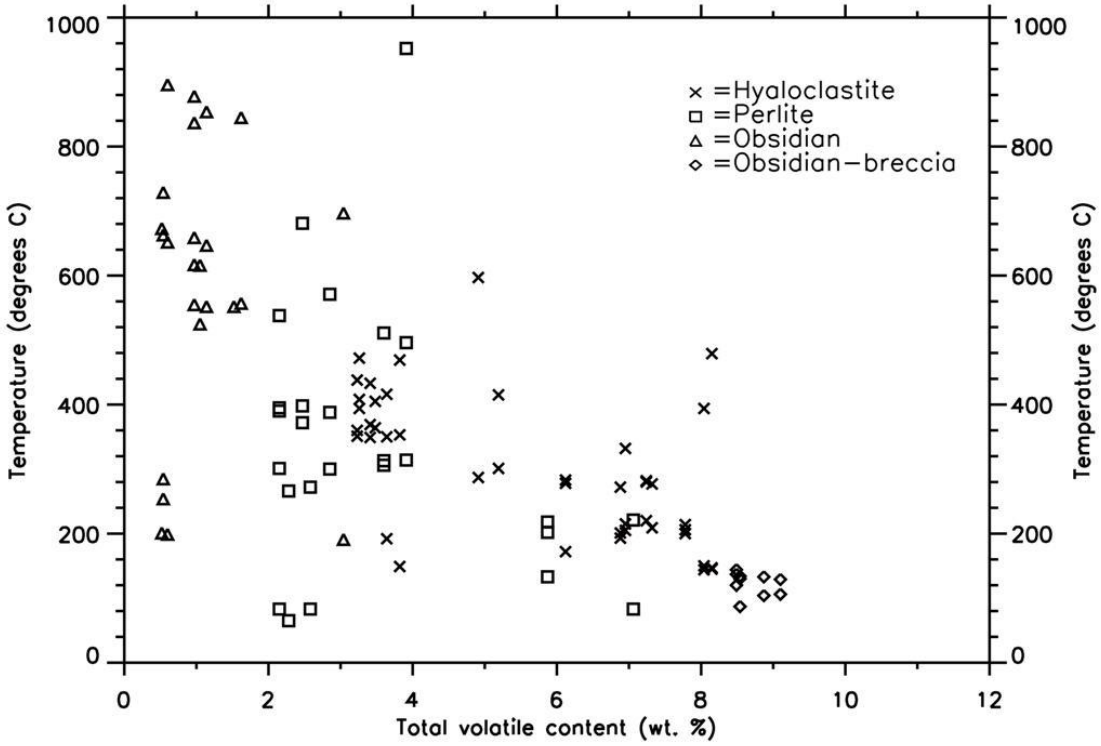
× =Hyaloclastite
□ =Perlite
△ =Obsidian
◇ =Obsidian−breccia
Temperature (degrees C)
Total volatile content (wt. %)
0
200
400
600
800
1000
0
2
4
6
8
10
12

1326 Fig. 5

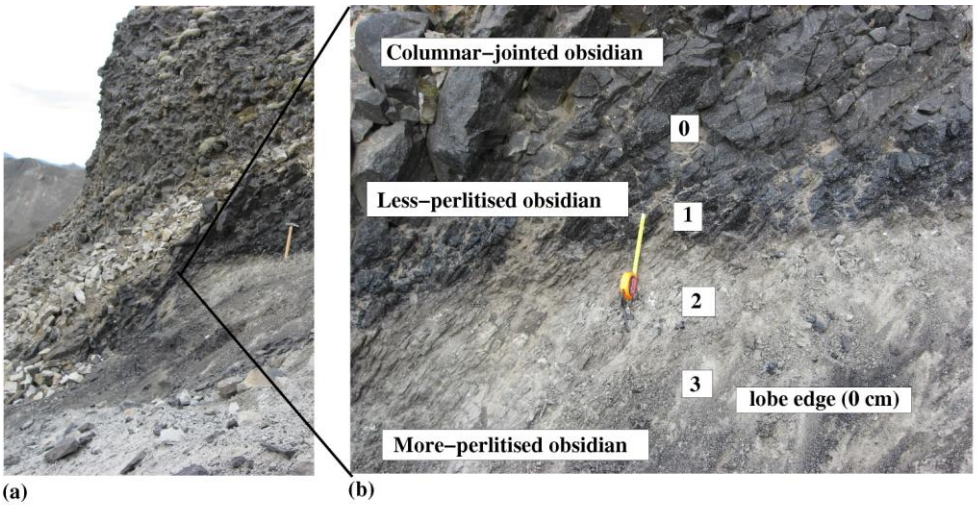
Columnar–jointed obsidian
0
Less–perlitised obsidian
1
2
3
lobe edge (0 cm)
More–perlitised obsidian
(a)
(b)

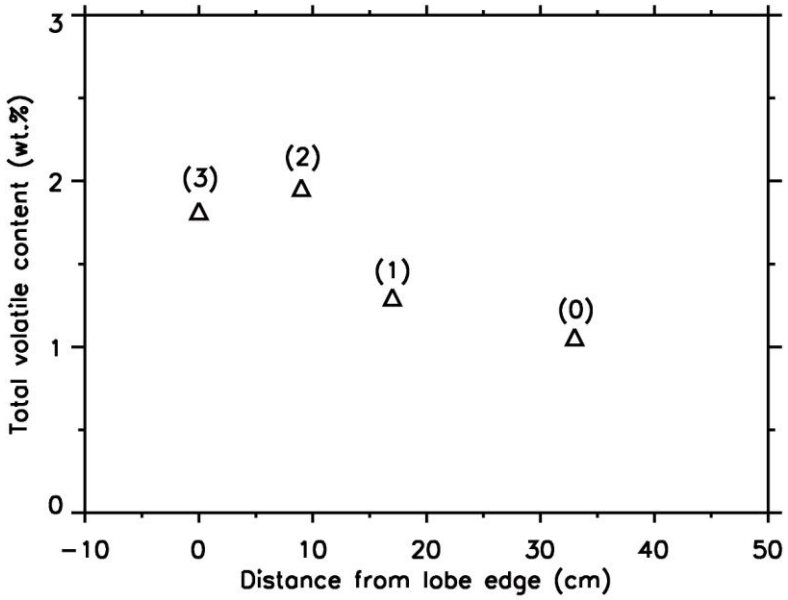
Total volatile content (wt.%)
Distance from lobe edge (cm)
(3)
(2)
(1)
(0)
3
2
1
0
−10
0
10
20
30
40
50

(c)

1327 Fig. 6

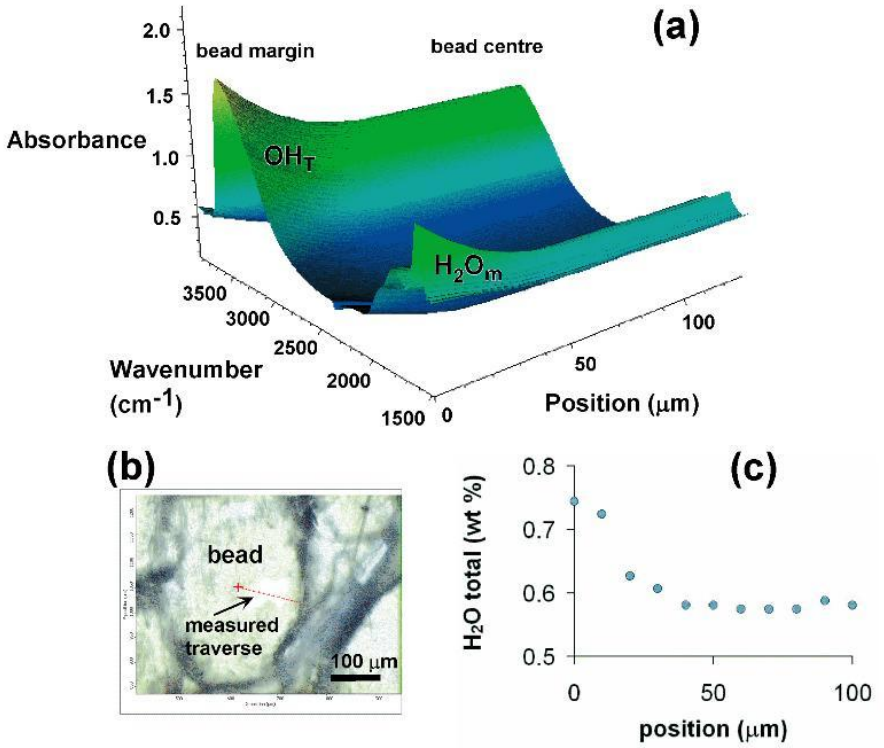
(a)
bead margin
bead centre
Absorbance
2.0
1.5
1.0
0.5
OH_T
H_2O_m
3500
3000
2500
2000
1500
Wavenumber
(cm^{-1})
0
50
100
Position (μm)
(b)
bead
measured
traverse
100 μm
(c)
H_2O total (wt %)
0.8
0.7
0.6
0.5
0
50
100
position (μm)

1328 Fig. 7

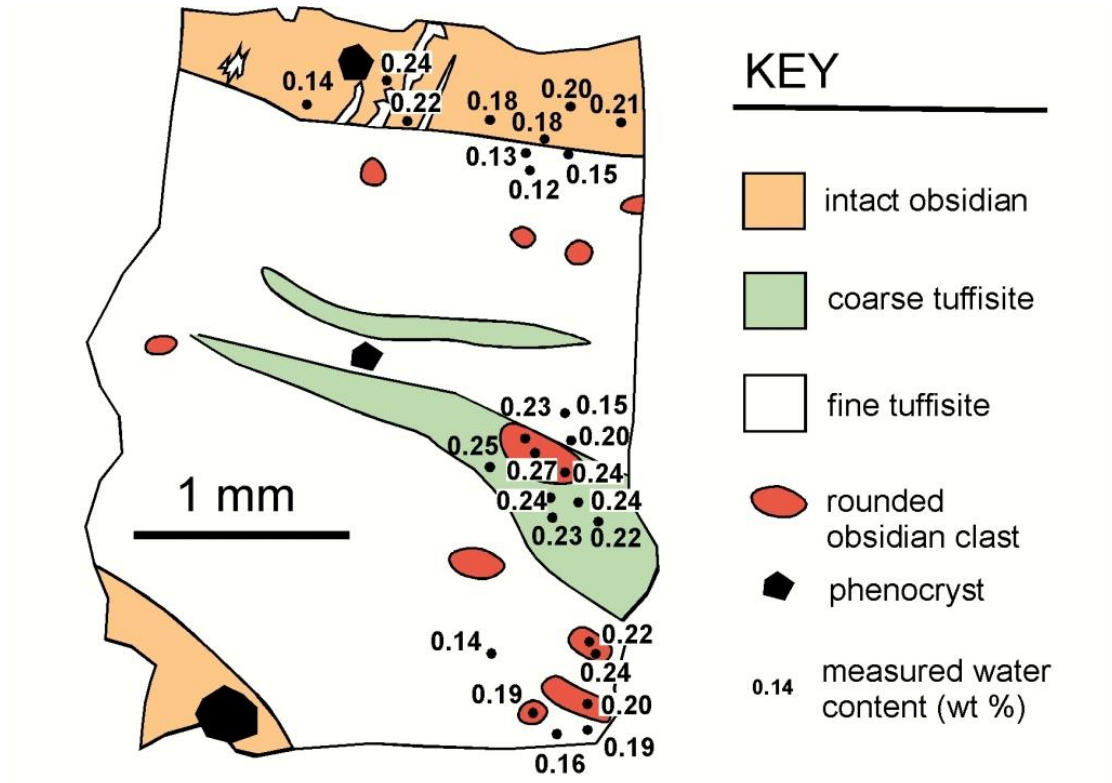
0.14
0.24
0.22
0.18
0.20
0.21
0.18
0.13
0.15
0.12
0.23
0.15
0.25
0.20
0.27
0.24
0.24
0.24
0.23
0.22
1 mm
0.14
0.22
0.24
0.19
0.20
0.19
0.16
KEY
intact obsidian
coarse tuffisite
fine tuffisite
rounded obsidian clast
phenocryst
0.14
measured water content (wt %)

1329 Fig. 8
1330
1331

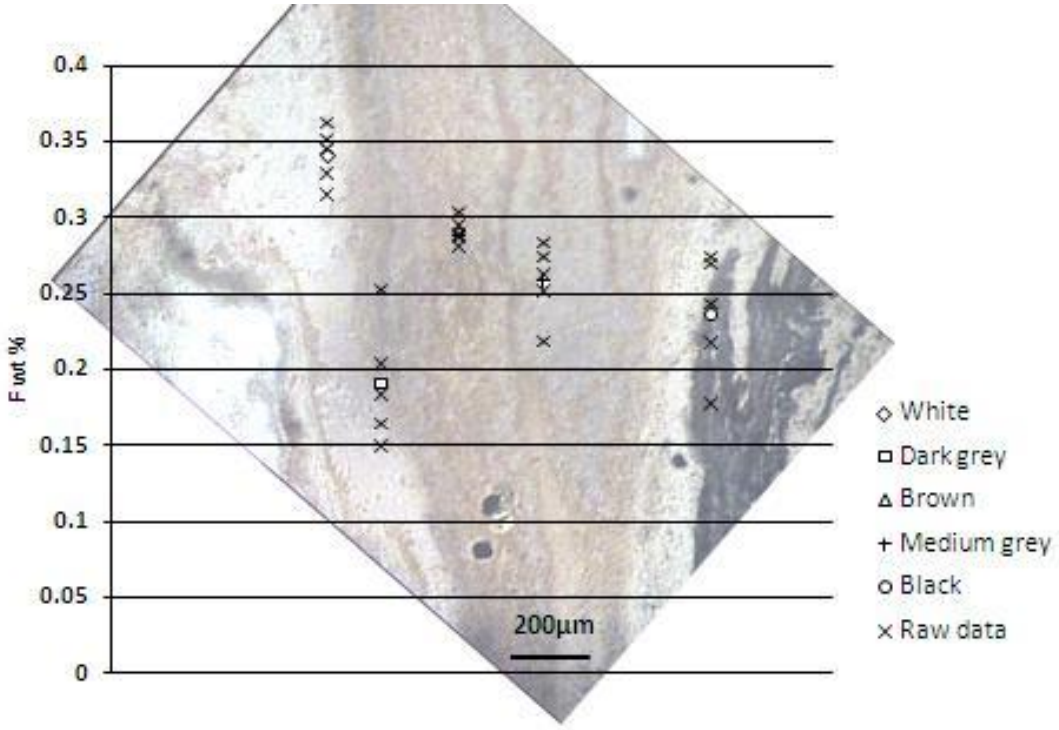

Fig. 9

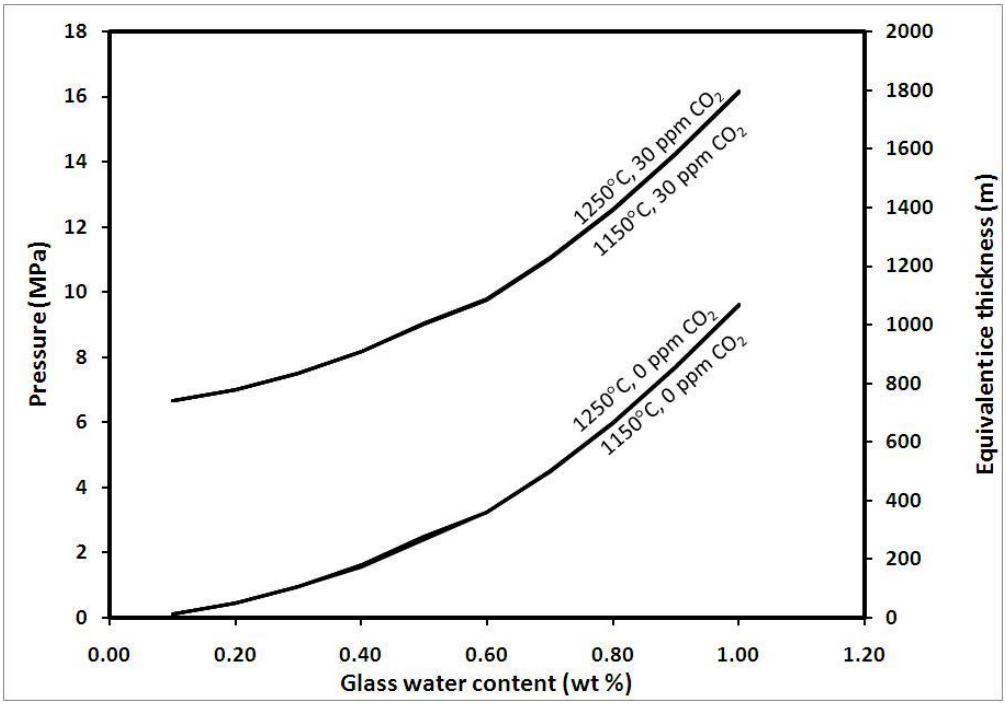
Pressure (MPa)
Equivalentice thickness (m)
Glass water content (wt %)
1250°C, 30 ppm CO2
1150°C, 30 ppm CO2
1250°C, 0 ppm CO2
1150°C, 0 ppm CO2
0
2
4
6
8
10
12
14
16
18
0
200
400
600
800
1000
1200
1400
1600
1800
2000
0.00
0.20
0.40
0.60
0.80
1.00
1.20

(a)

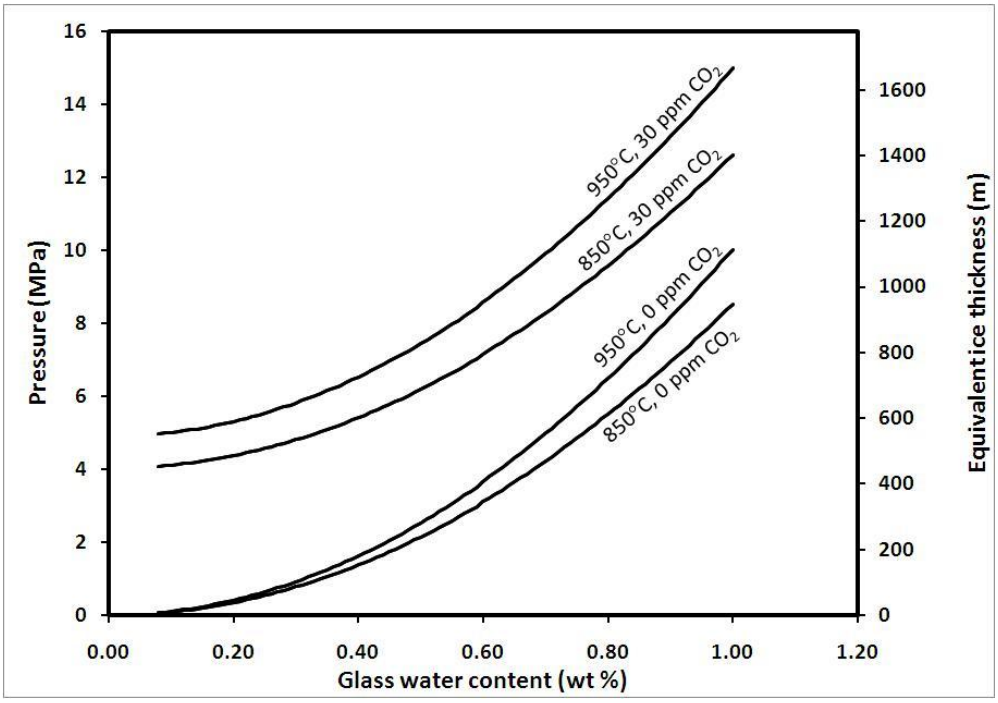
Pressure (MPa)
Equivalentice thickness (m)
Glass water content (wt %)
950°C, 30 ppm CO2
850°C, 30 ppm CO2
950°C, 0 ppm CO2
850°C, 0 ppm CO2
0
2
4
6
8
10
12
14
16
0
200
400
600
800
1000
1200
1400
1600
0.00
0.20
0.40
0.60
0.80
1.00
1.20

(b)

1343 **Fig. 10**

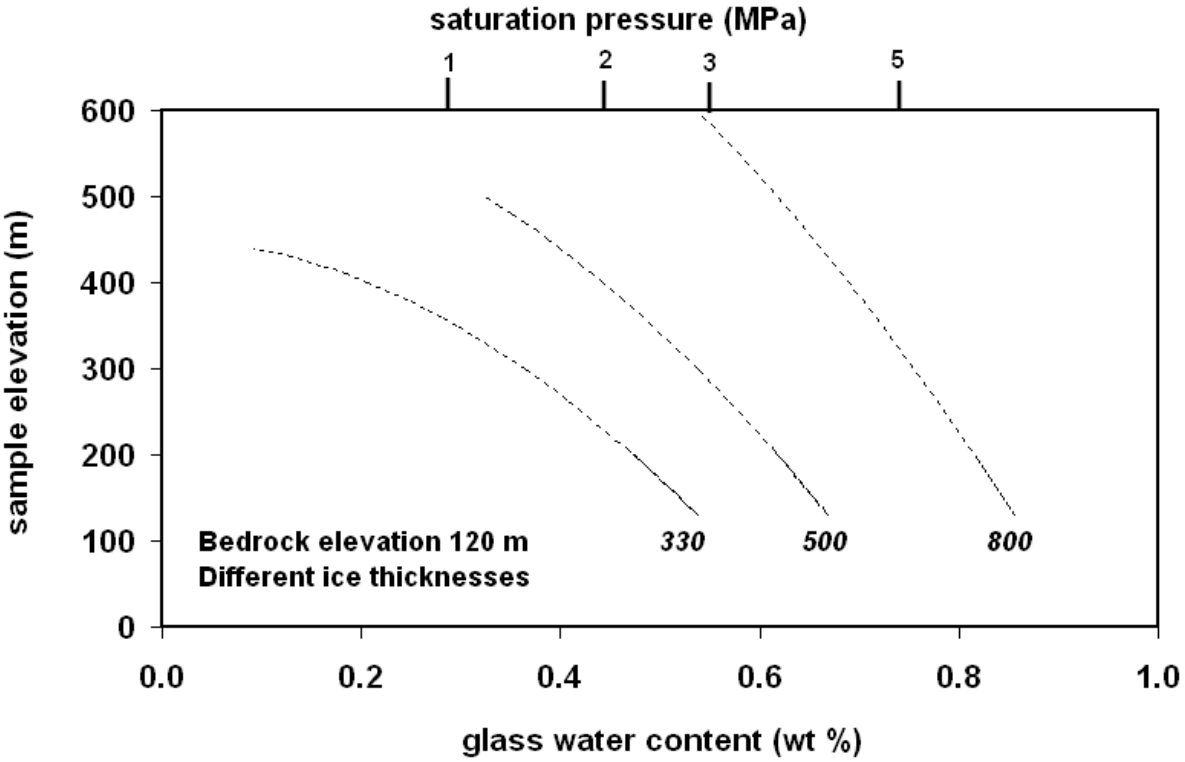

1344
1345

Figure 11

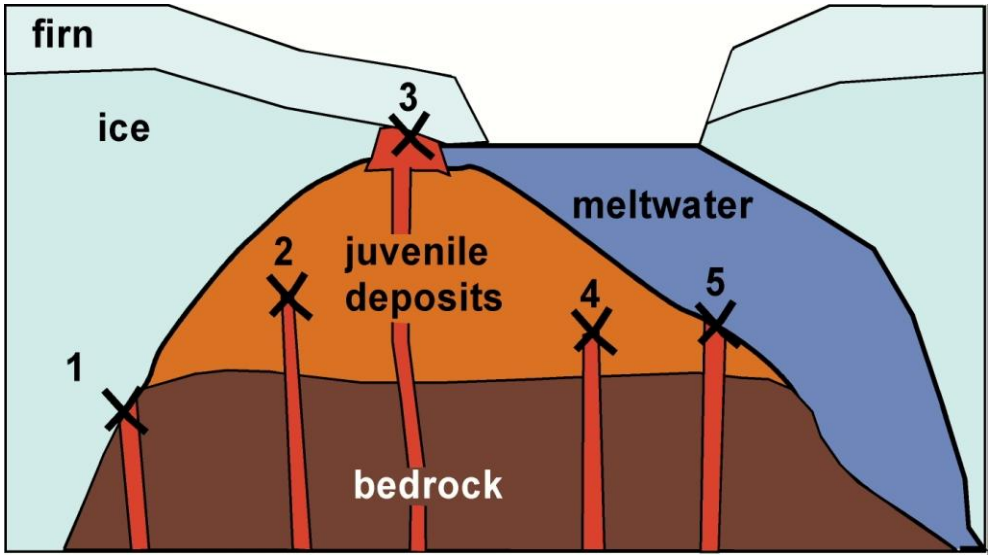
firn
ice
3
meltwater
2
juvenile
deposits
4
5
1
bedrock

(a)

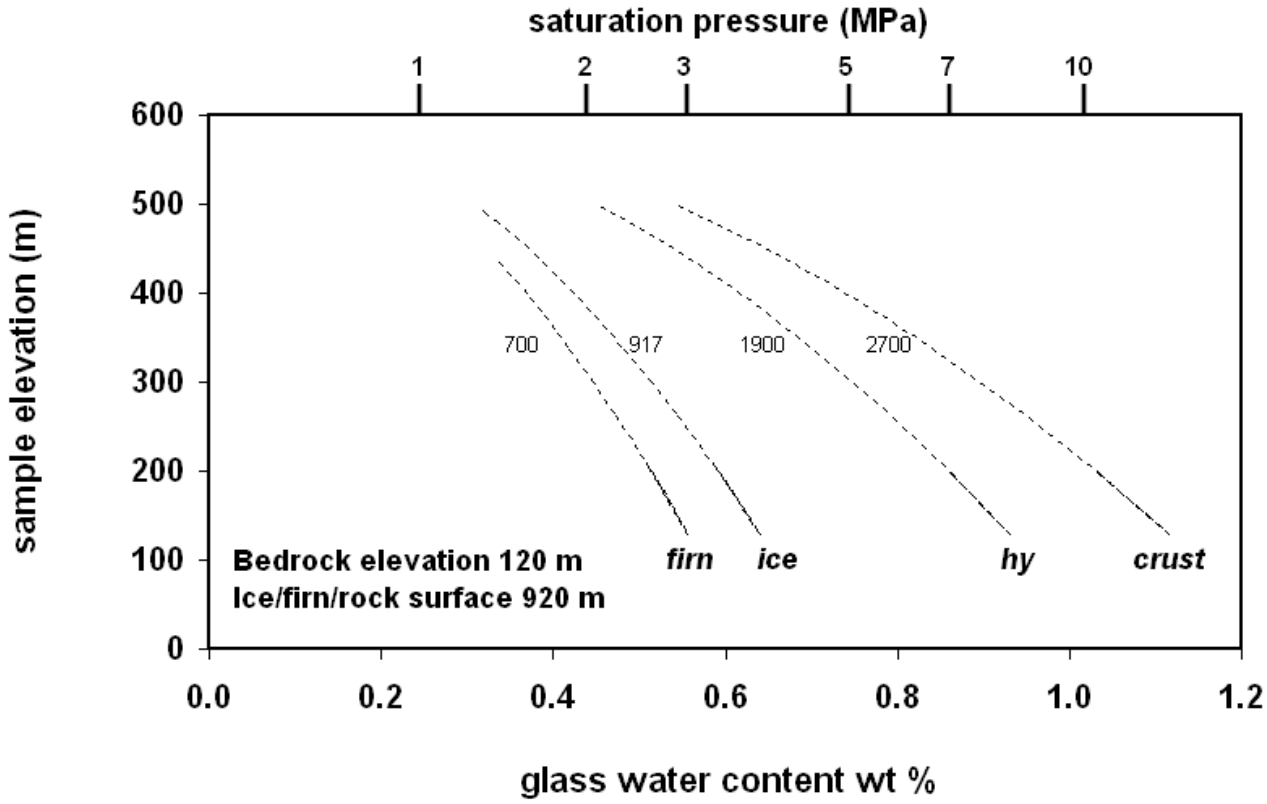
saturation pressure (MPa)
1
2
3
5
7
10
600
500
400
300
200
100
0
sample elevation (m)
700
917
1900
2700
Bedrock elevation 120 m
Ice/firn/rock surface 920 m
firn
ice
hy
crust
0.0
0.2
0.4
0.6
0.8
1.0
1.2
glass water content wt %

(b)

1383
1384 Fig. 12

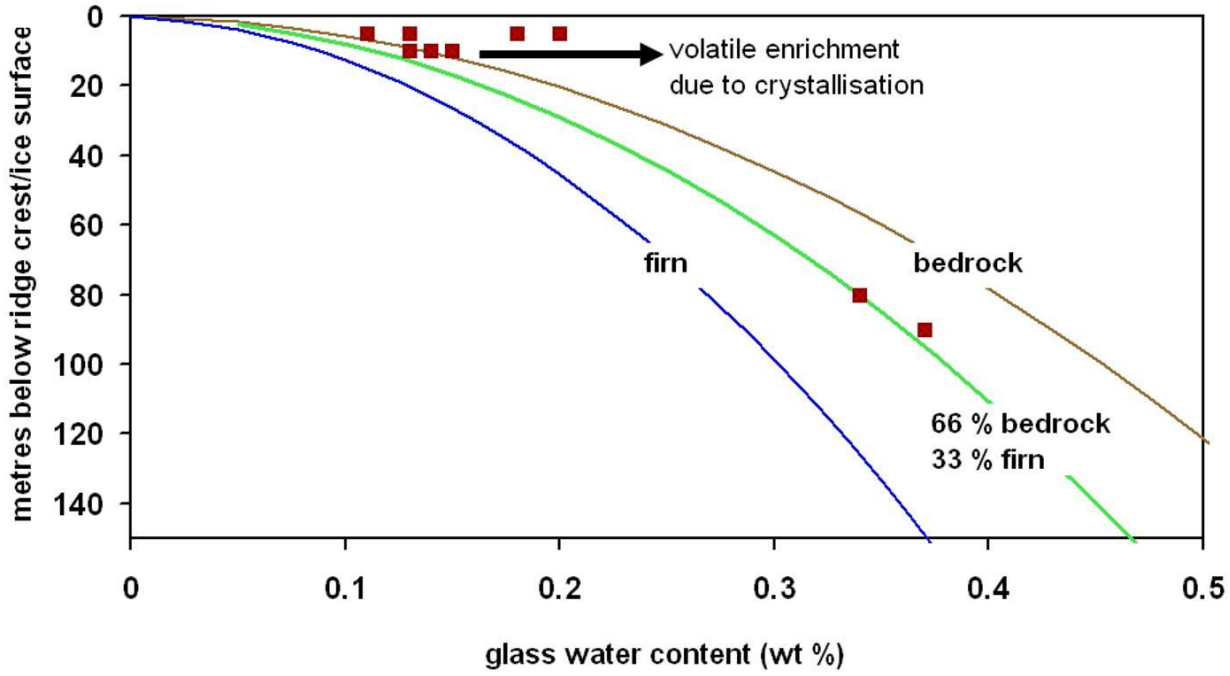

1385 Fig. 13
1386
1387
1388

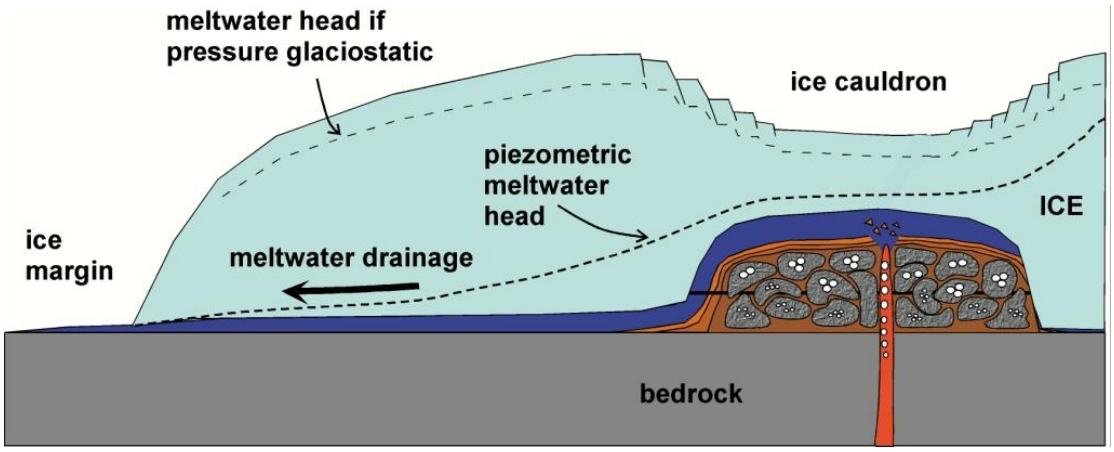

1389
1390
1391
1392 (a)
1393

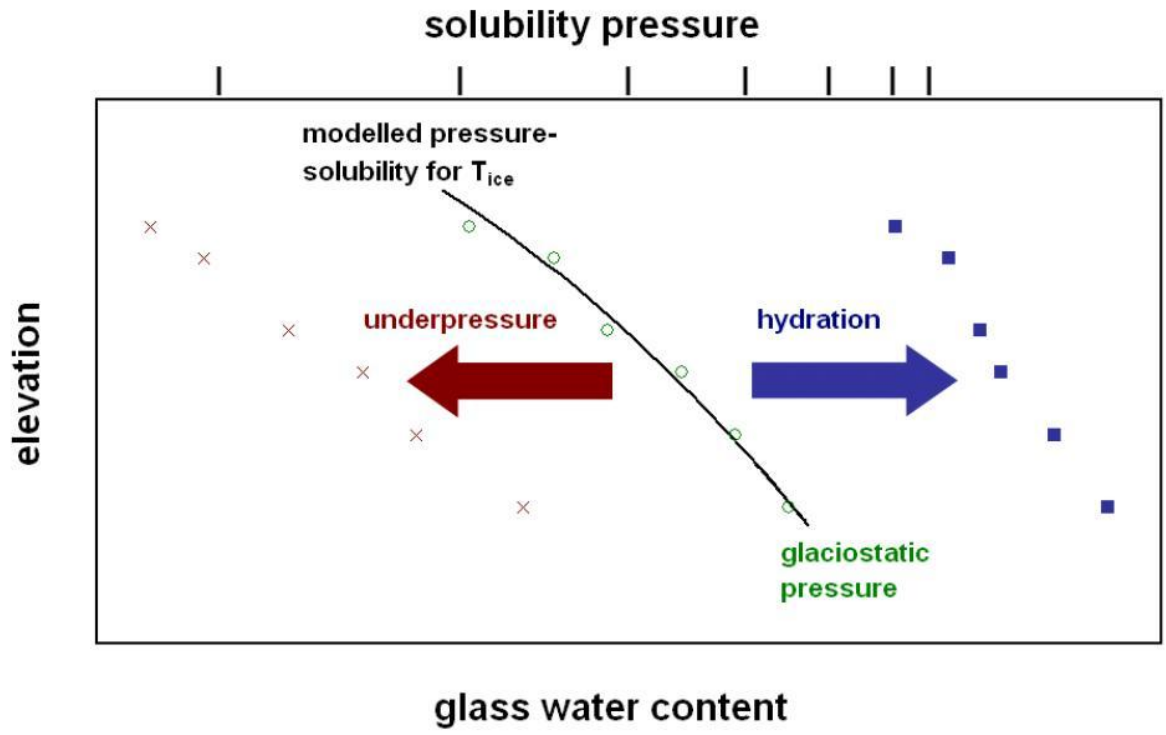

1394
1395 (b)

1396 Fig. 14

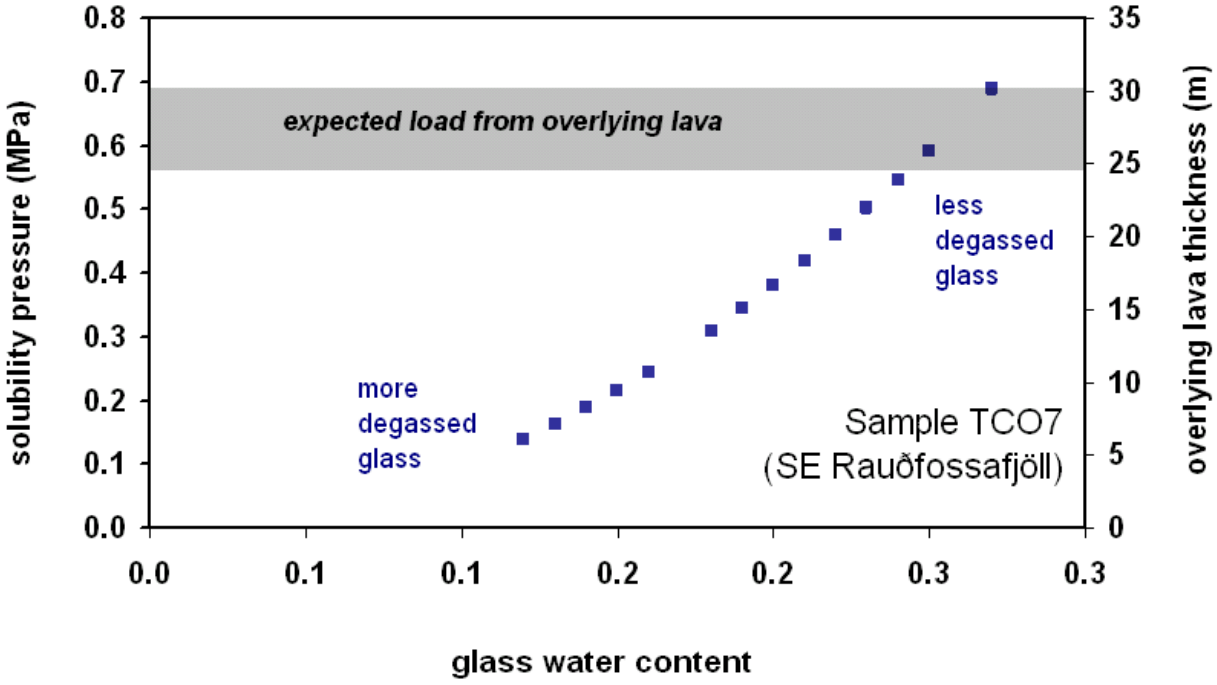

1397
1398

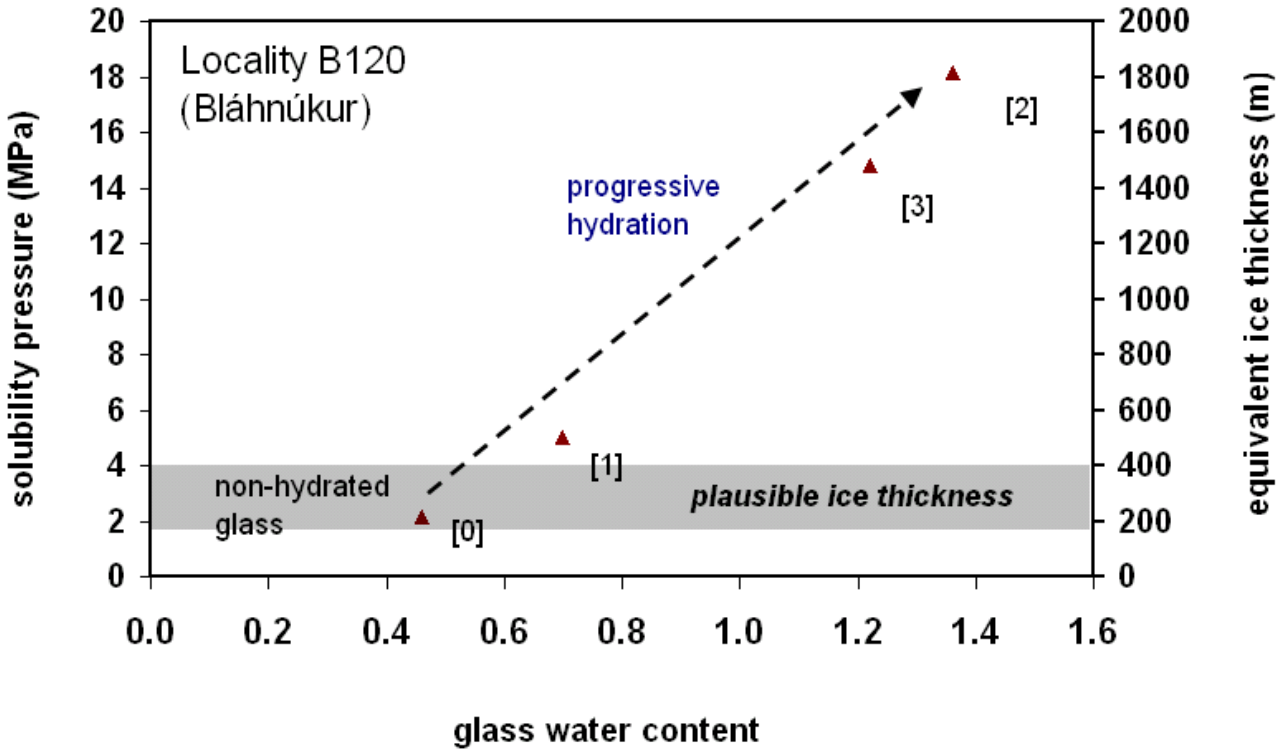

1399

1400 Fig. 15
1401
1402

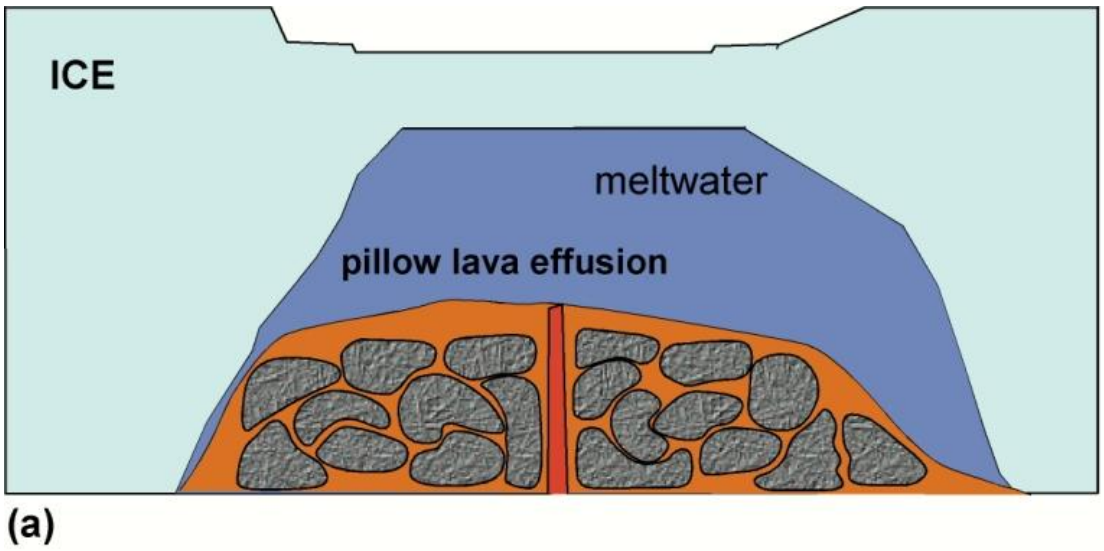

(a)

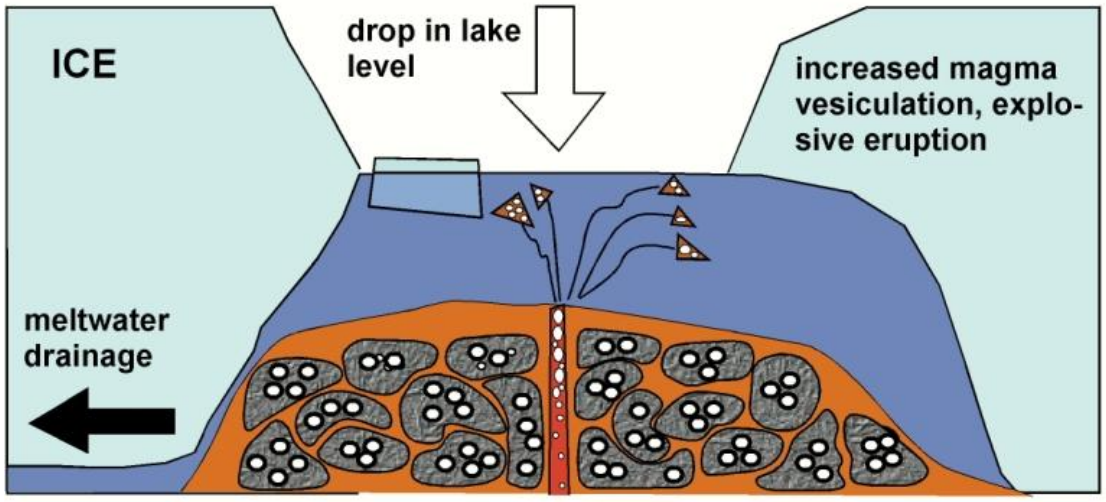

(b)

1403 vesiculation of pillow lavas

1404 TABLES
1405

Study	Location, magma type, eruption style	Volatiles measured	H_2O values	Other species	Inferred quenching pressures in MPa; (T_{ice})	Interpretation
Moore and Calk 1991	Various locations in Iceland, tholeiitic basalt, tuyas	S	---	S 800 ppm (basal pillows), <200 ppm (subaerial lavas)	---	S progressively degasses upwards, post-quenching movement causes deviations from trend
Moore et al. 1995	Ash Mountain, South Tuya and Tuya Butte, British Columbia, tholeiitic to alkali basalt, tuyas	H_2O, S	0.5 wt % (basal pillows) 0.2 wt % (subaerial lavas)	S 1000 ppm (basal pillows), 300-700 ppm (subaerial lavas)	---	Depressurisation during edifice construction led to tholeiitic-alkalic transition. Pillows not degassed, subaerial lavas partly degassed
Dixon et al. 2002	Tanzilla Mountain, British Columbia, tholeiitic to alkali basalt, englacial pillow-hyaloclastite edifice	H_2O, CO_2, S, Cl	0.56 - 0.63 wt %	CO_2 < 30 ppm S 870-1110 ppm Cl 280-410 ppm	3.6-8.1 (400-900 m) [3,4]	Tholeiites not degassed, alkali basalts degassed Consistent with other evidence for T_{ice}
Nichols et al. 2002	Iceland, basaltic pillow lavas from tuyas, tindars and pillow ridges	H_2O	0.10-1.02 wt %, greatest in central Iceland	---	---	Water-rich glass in central Iceland indicates a wet mantle plume
Schopka et al. 2006	Helgafell, Iceland, tholeiitic basalt, explosive tindar eruption	H_2O	0.26-0.37 wt %	---	0.8-1.6 MPa (90-180 m) [1]	Low quenching pressures require underpressure due to meltwater drainage
Hoskuldsson et al. 2006	Kverkfjoll, Iceland, tholeiitic basalt, pillow ridges and tindars	H_2O	0.85-1.04 wt %.	---	20 ppm CO_2: 11.2-14.8 (1240-1640 m) 30 ppm CO_2: 13.3-16.9 (1480-1880 m) [3]	Vesiculation of pillows due to meltwater drainage, 4.4-4.7 MPa pressure drop
McGarvie et al. 2007	Prestahnúkur, Iceland, rhyolite, lava-dominated englacial edifice	H_2O	0.10-0.14 wt % (lavas flowed down edifice flanks)	CO_2 < 30 ppm	---	Lavas degassed to near-atmospheric pressure, then flowed downslope beneath the ice

Tuffen et al. 2008	Dalakvisl, Torfajökull, Iceland, explosive-intrusive rhyolitic eruption	H_2O, F, Cl	0.50-0.52 wt % (obsidian sheets in pyroclastic deposit)	CO_2 < 30 ppm F 1600 ppm Cl 900-1000 ppm	0 ppm CO2; 3 (~350 m) 30 ppm CO2: 7 (~750 m) [1]	Partial degassing due to collapse of foam within pyroclastic deposit in subglacial cavity
Edwards et al. 2009	Mt Edziza, British Columbia, englacial pillow ridge	H_2O, CO_2*, S, Cl	0.54- 0.81 wt.%.	CO_2 < 30 ppm but 25 ppm at Tennena Cone* S 2000-2200 ppm Cl 400-500 ppm	0 ppm CO_2: 2.9-6.2 (296-628 m) 25 ppm CO_2: 8.7-11.7 (722-1302 m) [1,2]	Gentle pillow effusion due to high confining pressure. Large variations in level of ice-confined lake during edifice construction
Stevenson et al. 2009	Kerlingafjöll, Iceland, andesitic to dacitic, subglacially erupted tuffs and hyaloclastites	H_2O, CO_2	0.67-1.32 wt %	CO_2 < 30 ppm	0 ppm CO_2: 5.0 (556 m) 25 ppm CO_2: 7.5 (834 m) Sample with 1.32 wt % water ignored as intruded into hyaloclastite	Anomalously high volatile content due to intrusion into hyaloclastite, ice thicknesses consistent with facies
Tuffen and Castro 2009	Hrafntinnuhryggur, Krafla, Iceland, tholeiitic rhyolite, erupted through thin ice	H_2O, CO_2	0.11-0.37 wt % Feeder dyke 0.34-0.37 wt %, subaerial flow top 0.11-0.20 wt %	CO_2 < 30 ppm	Maximum from feeder dyke: 1.3 (140 m ice, 190 m firn at 700 kgm^{-3} or 55 m bedrock plus 35 m firn) [1]	Crystallisation causes volatile heterogeneity, quenching pressure of feeder dyke due to weight of firn + bedrock
Denton et al. 2009	Torfajökull and Krafla, Iceland, rhyolitic, variety of eruption types	Total volatiles (predominantly H_2O)	Total volatiles 0.44 wt % (subaerial lava) to 9.41 wt % (altered subglacial hyaloclastite)	F + Cl <0.5 wt %, CO_2 < 30 ppm	---	Extreme heterogeneity in water contents due to perlitisation and alteration

Table 1. Summary of previous studies of volatiles in subglacially erupted glasses. H_2O and CO_2 were measured using infra-red spectroscopy, whilst S, F and Cl were measured using electron microprobe, except *where CO_2 measured by manometry. Unless otherwise stated calculated ice thicknesses assume CO_2 has entirely degassed. Solubility-pressure relationships were calculated using [1] VolatileCalc (Newman and Lowenstern, 2002), [2] Moore et al. (1998) and [3] from Dixon and Stolper (1995) and Dixon et al. (1997).

Sample	Distance from lobe edge (cm)	Initial sample mass (mg)	Weight loss upon heating (wt. %)
B120 3	33	51.72	1.82
B120 2	17	52.04	1.96
B120 1	9	48.07	1.3
B120 0	Lobe edge (0cm)	44.70	1.06

Table 2. Total volatile content of variably hydrated rhyolitic obsidian at the margin of a lava lobe at Bláhnúkur, Iceland

1417 **Table 3.** Electron microprobe data for rhyolitic obsidian of sample J2 from Bláhnúkur, Iceland.
1418

Sample	W1	W2	W3	W4	W5	DG1	DG2	DG3	DG4	DG5	Br1	Br2	Br3
SiO_2	73.18	72.54	72.96	72.89	72.97	74.10	74.24	73.94	73.69	72.97	72.57	72.77	73.29
TiO_2	0.19	0.18	0.21	0.24	0.20	0.23	0.21	0.22	0.25	0.24	0.17	0.21	0.20
Al_2O3	14.24	14.17	14.35	14.05	14.21	13.77	14.02	14.01	13.88	14.08	13.95	14.09	14.21
FeO_T	2.46	2.59	2.46	2.43	2.58	2.59	1.93	2.32	2.18	2.94	2.54	2.72	2.43
MnO	0.09	0.05	0.09	0.09	0.10	0.06	0.05	0.04	0.03	0.08	0.09	0.08	0.05
MgO	0.17	0.11	0.14	0.16	0.13	0.08	0.03	0.01	0.07	0.18	0.11	0.08	0.08
CaO	0.62	0.59	0.66	0.60	0.63	0.66	0.35	0.33	0.47	1.11	0.41	0.36	0.40
P_2O_5	0.01	0.01	0.02	0.01	0.02	0.02	0.01	0.02	0.02	0.01	0.01	0.01	0.01
Na_2O	5.51	5.52	5.61	5.48	5.56	6.10	6.33	5.76	6.01	6.20	5.75	5.52	5.59
K_2O	5.13	5.29	5.20	5.21	5.38	4.14	4.03	4.76	4.34	3.92	5.11	5.29	5.33
F	0.35	0.32	0.33	0.35	0.36	0.16	0.18	0.25	0.20	0.15	0.28	0.30	0.29
Cl	0.18	0.18	0.18	0.17	0.17	0.17	0.19	0.21	0.17	0.12	0.19	0.19	0.18
Total	102.16	101.58	102.19	101.69	102.31	102.09	101.58	101.87	101.33	102.02	101.19	101.63	102.04

Sample	Br4	Br5	MG1	MG2	MG3	MG4	MG5	Bl1	Bl2	Bl3	Bl4	Bl5
SiO_2	73.75	73.15	73.31	73.32	73.02	73.32	73.42	72.88	72.56	72.31	72.85	73.03
TiO_2	0.17	0.20	0.24	0.21	0.22	0.20	0.19	0.25	0.24	0.21	0.21	0.21
Al_2O3	13.85	14.06	14.29	14.22	14.64	14.49	14.24	14.07	14.02	14.07	13.84	14.30
FeO_T	2.17	2.16	2.27	2.22	1.88	2.24	2.12	2.80	2.70	2.94	2.90	2.65
MnO	0.05	0.09	0.06	0.06	0.06	0.05	0.04	0.08	0.11	0.09	0.09	0.08
MgO	0.01	0.08	0.04	0.00	0.05	0.01	0.06	0.11	0.14	0.17	0.17	0.14
CaO	0.40	0.42	0.25	0.27	0.54	0.32	0.34	1.02	0.86	0.66	0.66	0.90

P_2O_5	0.01	0.02	0.01	0.02	0.01	0.01	0.02	0.02	0.01	0.02	0.01	0.02
Na_2O	5.66	5.47	5.55	5.68	6.47	5.76	5.70	6.05	5.64	5.57	5.49	5.91
K_2O	4.92	5.24	5.11	5.32	4.25	5.09	5.27	4.29	4.93	5.08	5.31	4.47
F	0.29	0.30	0.25	0.26	0.22	0.27	0.28	0.18	0.24	0.27	0.27	0.22
Cl	0.18	0.19	0.20	0.19	0.14	0.17	0.19	0.14	0.17	0.19	0.17	0.15
Total	101.48	101.38	101.59	101.77	101.53	101.97	101.89	101.91	101.64	101.59	101.99	102.07

1419
1420